R-05-66

Sm-Nd isotope determinations of low-temperature fluorite-calcite-galena mineralization in the margins of the Fennoscandian Shield

Report of activities carried out during 2004

E Alm, Department of Geology and Geochemistry, Stockholm University

K Sundblad, Department of Geology, Turku University, Finland

H Huhma, Geological Survey of Finland, Espoo, Finland

November 2005

Svensk Kärnbränslehantering AB
Swedish Nuclear Fuel
and Waste Management Co
Box 5864
SE-102 40 Stockholm Sweden
Tel 08-459 84 00
+46 8 459 84 00
Fax 08-661 57 19
+46 8 661 57 19

ISSN 1402-3091
SKB Rapport R-05-66

Sm-Nd isotope determinations of low-temperature fluorite-calcite-galena mineralization in the margins of the Fennoscandian Shield

Report of activities carried out during 2004

E Alm, Department of Geology and Geochemistry,
Stockholm University

K Sundblad, Department of Geology,
Turku University, Finland

H Huhma, Geological Survey of Finland,
Espoo, Finland

November 2005

Abstract

A significant and widely distributed system of Phanerozoic low-temperature fluorite-calcite-galena mineralization is known along the margins of the Fennoscandian Shield. It occurs as narrow veins in the Precambrian crystalline basement or as pore fillings in Vendian to Lower Cambrian sandstones, in both cases without any known association to igneous activity. The system has locally (Laisvall and Vassbo, along the Caledonian front) been of major economic interest and the genesis and age has been frequently discussed in the geoscientific literature for more than fifty years. Major problems addressed in these publications have been sources, transport and depositional mechanisms of the fluids as well as timing, the latter including Cambrian, Silurian and Permian alternatives. The occurrence of a similar hydrothermal system in the Baltic Sea region, thus recognizing an even wider perspective for this system, has been reported in a previous report to SKB /Alm and Sundblad 2002/.

The current report concerns the first effort to date the hydrothermal system by applying the Sm-Nd isotope method on fluorite (and calcite). For this purpose, four target areas were selected: Götemar and Tindered in southeastern Sweden, Lovisa in southeastern Finland and Laisvall in northern Sweden. Of these target areas, Götemar, Tindered and Lovisa represent vein mineralization along the southeastern margin of the Fennoscandian Shield and Laisvall sandstone-hosted mineralization along the Caledonian front.

The results indicate local variations in the initial $^{143}Nd/^{144}Nd$ ratios, which influence negatively on the possibility to date this system. Nevertheless, individual fluorite (and calcite) populations, representing well-defined geological environments, display linear trends that have been evaluated with respect to ages. The most reliable and precise ages were obtained by analyzing coprecipitated mineral pairs (fluorite and calcite). Sm-Nd isotope age calculations, using other geologically relevant sample populations, resulted in similar ages, although with less precision, in all cases indicating hydrothermal activity in the Silurian to Early Devonian. This activity took place in conjunction with major fracture and fault tectonics reaching many hundreds of metres below the subcambrian peneplain.

Comparison with well-dated lead mobilization in the interior of the Caledonides and K-feldspar overgrowths in the Caledonian front suggest that the hydrothermal activity in the Caledonides took place at 420–430 Ma (Wenlock/Ludlow). Comparison with well-dated regional fracture systems in Latvia suggest that the low-temperature hydrothermal veins in the Baltic Sea region were formed in conjunction with faulting, uplift and the transition from marine to fluvial sedimentary conditions during the Lochkovian to Pragian, i.e. at c 410–415 Ma, some 5–10 m.y. later than the hydrothermal event in the Caledonides. The time lag between the hydrothermal activity in these two environments is in accordance with sedimentological evidence for a southeastwards migrating Caledonian thrust front during the Late Silurian to Early Devonian.

Contents

1 Introduction

The investigation reported here is an attempt to constrain the age of a significant and extensive low-temperature hydrothermal system, which is identified as fluorite-calcite-galena-mineralization in veins and sandstones in the marginal parts of the Fennoscandian Shield. This hydrothermal system has been described with respect to geological setting, mineral paragenesis, fluid inclusions and lead isotope systematics by different authors; along the Caledonian front by e.g. /Rickard et al. 1979, Lindblom 1982, Johansson 1983/ and in the Baltic Sea region by /Alm and Sundblad 2002/.

Four criteria need to be fulfilled for formation of these mineralizations; 1) a source rock with easily accessible elements to be released by a hydrothermal fluid, 2) a high enough temperature to generate a hydrothermal convecting system, 3) intense fracturing to provide channels for the fluid, or, in the case of sandstone, adequate channelways from the source to the site of deposition and 4) physico-chemical conditions that trap dissolved components on the channel walls or in the pore space of the sandstone. Relatively well-established models for the sandstone-hosted mineralizations are available in the literature but the potential relation between sandstone-hosted mineralization and vein mineralization is never proven and the age of the latter largely unknown, apart from a lower age limit at the beginning of the Phanerozoic. This is one reason why age determinations are critical for this system. A second reason is that if a common model for these mineralized systems can be established, it would imply that shield-scale tectonic-hydrothermal reactivation of the Precambrian crust has occurred at some Phanerozoic event, which is of fundamental importance when discussing long-term deposition of radioactive waste material.

The present study is unique in that it is the first attempt to determine the age of Fennoscandian fluorite (and calcite) by the Sm-Nd isotope method and it has thus involved both method development and a result-oriented approach. It has been carried out in two phases; during phase 1, fluorite (and calcite) from hydrothermal vein systems in three target areas in the Baltic Sea region – Götemar, Tindered, and Lovisa – were collected and analyzed for isotopic composition. The results were presented in an SKB report /Alm et al. 2004/ and also presented publicly as a key note lecture at an international symposium in Helsinki, September 2004 /Sundblad et al. 2004/. Since the results reported in 2004 indicated that the age estimates of fluorites could be improved if the isotope data were supplemented by adequate Sm-Nd data for the potential source rocks to the fluorites, relevant rock samples in each of the three target areas were collected for phase 2 of the study. Furthermore, a fourth target area, namely Laisvall with sandstone-hosted fluorite and galena, was included.

2 Geological background

2.1 General geological evolution of Fennoscandia, with particular emphasis on the Late Precambrian and the Palaeozoic

The Fennoscandian Shield is the largest exposed segment of Precambrian crust in Europe. It includes numerous crustal segments of highly variable compositions and ages, formed at discrete steps during the Archaean and Proterozoic by a number of geological processes /Gaál and Gorbatschev 1987/. The c 3,500 Ma trondhjemitic gneisses /Huhma et al. 2004/ constitute the oldest crustal units and the c 900 Ma post-Sveconorwegian granites the youngest. As a result of this prolonged crustal evolution, the continent Baltica was established in the Neoproterozoic, by that time linked to Laurentia in the supercontinent Rodinia. After the Sveconorwegian orogenic event, Baltica was subject to denudation that created a subcambrian peneplain over large parts of Fennoscandia /Lidmar-Bergström 1996/. These denudation processes were soon (c 800–750 Ma) accompanied by extensional tectonics and intracratonic basin evolution, which paved the way for the opening of the Iapetus Ocean between Baltica and Laurentia in the Early Vendian /Kumpulainen and Nystuen 1985, Vidal and Moczydlowska 1995, Nikishin et al. 1996/. As a result, marine transgression took place over vast areas of the subcambrian peneplain and eventually, formation of oceanic crust between Laurentia and Baltica was initiated. Three distinct geological environments thus developed in the Vendian and Early Palaeozoic, prior to the Caledonian continent-continent collision with associated orogenic overprints; eugeoclinal deposition in the Iapetus Ocean, miogeoclinal deposition along the present western edge of Baltica and shallow-marine deposition in an epicontinental sea further to the east.

2.1.1 Eugeoclinal evolution

Tholeiitic dolerites, intruding into quartzo-feldspathic sedimentary rocks along the continental margin of Baltica at 665 Ma /Claesson and Roddick 1983/, and into similar continent-derived sedimentary rocks at 608 Ma /Svenningsen 2001/, constitute the earliest magmatic evidence of incipient seafloor spreading in the Iapetus Ocean. The main formation of juvenile crust occurred during the Late Cambrian and the Ordovician when the distance between Baltica and Laurentia was at its largest. Island arcs formed at c 490 Ma /Claesson et al. 1988/, and ophiolites at c 490 Ma and 440 Ma /Dunning and Pedersen 1988/. The Iapetus Ocean began to close in the Late Ordovician when Baltica collided with the microplate Avalonia /Stephens and Gee 1989/. The final closure began in the Wenlockian-Ludlowian, when Baltica (and Avalonia) collided with Laurentia, and was completed in the earliest Devonian. Baltica was overridden by Laurentia, resulting in nappe transport towards the southeast on Baltica /Stephens and Gee 1989, Torsvik et al. 1996/. The eugeoclinal successions are now preserved as exotic terranes in the Upper Allochthon of the Scandinavian Caledonides.

2.1.2 Miogeoclinal evolution

Marine sedimentation took place along the western continental slope of Baltica throughout the Vendian, Cambrian, Ordovician and Early Silurian, giving rise to quartzites, shales and limestones as well as high-energy turbidite deposits /Kumpulainen and Nystuen 1985, Bassett 1985/. These shallow-marine conditions prevailed until the Wenlockian, when

the marine successions conformably were overlain by Late Silurian fluvial siliciclastic sediments, as documented from the allochthonous Röde Formation in the central Swedish Caledonides /Bassett et al. 1982/. The Röde Formation is interpreted to represent a distal facies of Old Red sandstone, derived from the advancing Caledonian nappes as an immediate response to the continent-continent collision between Laurentia and Baltica /Bassett et al. 1982/. The miogeoclinal deposits are now preserved as thrust sheets in the Lower and Middle Allochthon of the Scandinavian Caledonides.

2.1.3 Epicontinental evolution

The early sedimentary evolution in the central and eastern parts of Fennoscandia (the Baltoscandian epicontinental sea) was more tranquil and generated Vendian to Early Cambrian sandstones and Middle to Late Cambrian organic-rich alum shales /Bergström and Gee 1985, Mens and Pirrus 1997/. Early Cambrian sandstone is recognized also as dykes in the crystalline basement, immediately below the subcambrian peneplain /e.g. Mattsson 1962, Bergman 1982/. /Bergman 1982/ suggested that these clastic dykes were related to tectonic events causing earthquakes and that sand was injected into fractures from above during the Early Cambrian and Early Ordovician. Marine epicontinental conditions continued through the entire Ordovician and most of the Silurian with predominantly carbonate facies sedimentation /Bruton et al. 1985, Basset 1985, Nestor and Einasto 1997/. A sudden change in the sedimentary environment was first noted in the western parts of the basin, where a transition from Wenlockian marine limestones to Late Silurian fluvial siliciclastic deposits is documented from the autochthonous Ringerike Group in the Oslo region /Turner and Whitaker 1976/. Slightly later (latest Pridolian and earliest Lochkovian), a similar, but more dramatic, transition was recorded in the eastern parts of the basin due to rapid uplift and local erosion of all previous strata. As a result, the earliest Devonian strata (fluvial siliciclastic Old Red sediments and dolomites belonging to the Lochkovian Gargzdai group) were deposited on a marked unconformity /Kurss 1992, Kleesment and Mark-Kurik 1997, Murnieks 1999/. Deposition of the Gargzdai group was followed by more uplift and erosion, resulting in a new unconformity until dolomite-cemented siliciclastic sediments (Kemeri Formation) were deposited during the Pragian and Emsian. These Early Devonian successions were overlain by more fluvial sediments during the Middle Devonian and evaporitic and carbonate deposition prevailed during the Late Devonian. The epicontinental deposits are now preserved as autochthonous successions along the margins of the Fennoscandian Shield, with the most complete sections in the Baltic Sea region.

2.1.4 Development of a foreland basin and post-orogenic sedimentary basins

Stratigraphic and sedimentological evidence for a southeastwards migrating foreland basin in Fennoscandia in the Late Silurian/Early Devonian was first presented by /Bassett 1985/ based on data for a profile from the central Scandinavian Caledonides to northern Poland. This was further elaborated by /Kurss 1992/ who created a sedimentological model for the development of the Devonian Old Red sandstone basin in the entire North Atlantic region. Quantification of the dimensions of this foreland basin has given width estimates of 350 to 600 km and depth estimates ranging from 6.5 km in Jämtland to a few kilometres in south-central Sweden. This basin structure was accompanied by a foreland bulge in the Baltic Sea region or even further to the east /Middleton et al. 1996, Samuelsson and Middleton 1998, Larson et al. 1999/.

2.1.5 Tectonic aspects

The compressional event induced by the Caledonian continent-continent collision generated crustal thickening, partly due to the overriding of Laurentia on Baltica and partly due to nappe emplacement onto the northwestern margin of Baltica. The tectonic stress was accompanied by hydrothermal activity in the Precambrian granitic basement in the interior parts of the Caledonian orogeny, with mobilization of U and Pb at 420 Ma /Stuckless et al. 1982/. The compressional phase of the orogeny was succeeded by extensional tectonic conditions before the end of the Early Devonian /Fossen and Rykkelid 1992, Braathen et al. 2002/ resulting in listric faults and half-graben structures, accompanied by rapid erosion and deposition of km-thick Early to Middle Devonian sediments in intermontane basins on top of eroded, metamorphosed Caledonian crust /Hossack 1984, Steel et al. 1985, Norton et al. 1987/.

The rapid uplift and associated erosion of Early Palaeozoic strata in the Baltic Sea region, as well as the subsequent dramatic change in sedimentary environments in the beginning of the Devonian, was an immediate response to major fracturing and faulting of the Precambrian crust and overlying sedimentary successions. This is best seen in Latvia, where block movements with vertical displacements of up to 500 metres are documented along a set of ENE-trending faults that extend from the Baltic Sea to the Russian border /Brangulis and Kanevs 2002/. These faults affected the Precambrian crystalline basement, as well as the entire Cambro-Silurian and lowermost Devonian (Lochkovian) platform sediments, but are overlain by undisturbed Pragian and Emsian strata (Kemeri Formation) as well as younger Devonian strata, thus providing a Lochkovian/Pragian age of the faults; c 410–415 Ma, according to the time scale of /Gradstein et al. 2004/. A similar zone of fractures and faults is documented in Estonia, through the Precambrian basement and the Cambro-Silurian succession from Pärnu to Narva, i.e. along the Devonian front /Puura and Vaher 1997/. The Latvian and Estonian fault systems shall thus be seen in the perspective of the new stress field in the continental crust of Baltica, which was induced by the Caledonian event. It is worth noting that the Latvian faults follow the same structural trend as the docking zone between Baltica/Avalonia and Laurentia, as presented by /Torsvik et al. 1996/. The Latvian faults can thus have formed in response to a zone of weakness represented by the Laurentian/Avalonian margin that progressed into Baltica in the Lochkovian. A contemporary (Lochkovian) rift phase is also identified in the Pechora-Kolva basin in the northeastern part of Baltica /Nikishin et al. 1996/.

2.1.6 Carboniferous to Permian evolution

Lower Carboniferous sandstones, shales, siltstones and dolomites, followed by an unconformity and Upper Permian limestones, dolomites and sandstones are preserved in Latvia, Lithuania, the Kaliningrad region and northeastern Poland /Brangulis et al. 1998/ as well as in the Oslo region of southern Norway. This sedimentation was associated with significant tectonic and magmatic activity during the Late Carboniferous to Permian, when a failed intracontinental rift graben developed along a NNE-trending fracture in the Oslo region, with significant formation of alkaline intrusive and extrusive rocks /Neumann et al. 1992/. A NW-trending branch of the Oslo Palaeorift runs through the southernmost tip of Sweden (Skåne) and forms the present southwestern boundary of the Fennoscandian Shield and the entire East European Platform.

/Tullborg et al. 1995/ and /Larson and Tullborg 1998/ noted that the lower intercept for many U-Pb isochrons of Swedish Precambrian crustal units indicate disturbance of the isotopic systems and lead loss from the zircons in the Late Palaeozoic, mainly at 250–300 Ma, i.e. in the Permian. This was interpreted /Larson and Tullborg 1998/ to be due to elevated temperatures in the Precambrian crust caused by the thick overburden of Devonian sediments, conditions which were suggested to have remained for at least 100 m.y.

2.2 Geological setting of Phanerozoic fluorite-calcite-galena mineralization in the Fennoscandian Shield

Phanerozoic fluorite-calcite-galena mineralization is reported from a number of sites in the Precambrian crust of the Fennoscandian Shield. Two principal geological environments can be distinguished: 1. mineralizations associated with Permian igneous activity and 2. mineralizations that are unrelated to igneous activity. The latter group can be further subdivided into vein mineralization and sandstone-hosted mineralization.

1. Mineralizations connected with Permian igneous activity

Fluorite-calcite-galena-bearing veins, connected with Permian igneous activity, are reported from several sites in the Oslo region /see e.g. Bjørlykke et al. 1990/ as well as in the Skåne region /see e.g. Johansson and Rickard 1982/. Since it was concluded that the veins in the Baltic Sea region do not belong to this mineralization system /Alm and Sundblad 2002/, this group will not be discussed further in the present report.

2. Mineralizations unrelated to igneous activity

a. Veins

Fractures filled with calcite and/or fluorite and galena, without igneous association, are identified at a number of sites all over the Fennoscandian Shield /Johansson 1983, Alm and Sundblad 2002/ (Figure 4-1). They occur in the upper parts of the Precambrian crystalline basement, probably reaching a maximum depth of 1 km below the subcambrian peneplain and often in close spatial association to Cambrian sandstone dykes. The mineralized fractures are therefore mainly located along the margins of the shield or close to inliers of Palaeozoic sedimentary rocks underneath the Bothnian Sea and the Gulf of Bothnia. These vein mineralizations display open-space textures and occur in closely spaced (dm-m-scale) fracture systems, commonly with steeply dipping and NNE- to ENE-trending orientations, indicating a significant extensional tectonic event. The mineralized fractures show compositional variations, both with respect to paragenesis and lead isotopic compositions. Most fractures are dominated by calcite, others by fluorite and yet others (more rarely) by galena, but two or three of these phases commonly occur in various proportions at each locality. The most fluorite-rich veins are encountered where high F contents are recorded in the Precambrian host rocks (> 0.2% F), which indicates a rather local origin of the fluids. The lead isotopic composition of galena is variably radiogenic ($^{206}Pb/^{204}Pb$ ratios ranging from 17.0 to 35.0) and the lead isotopic signature for individual veins is characteristic for each host rock, supporting a local derivation of the fluids. Fluid inclusion data indicate vein formation under relatively shallow conditions from moderately saline, $CaCl_2$-dominated fluids and with depositional temperatures of 100–150°C. /Johansson 1983/ assumed a Caledonian age for the calcite veins but stated that his lead isotopic results were not conclusive enough to specify an exact age for the veins. /Tullborg et al. 1995/ and /Larson and Tullborg 1998/

suggested that the veins were formed in the Late Palaeozoic as a result of the accumulation of thick sequences of Devonian sediments on the Precambrian basement and related lead loss from zircons. Using the same frequency distribution of ages for the veins as /Larson and Tullborg 1998/ showed for the lower intercept ages of Precambrian zircons, the veins should mainly have formed during the time period from 250–300 Ma, i.e. in the Permian.

b. Sandstone-hosted galena-calcite-fluorite mineralization

Galena-calcite-fluorite mineralizations are also common as cement in Late Precambrian to Cambrian sandstones along the Caledonian front. Calcite is the most frequent mineral but accumulations of galena and fluorite are locally so intense that they represent a significant economic value, particularly at Laisvall and Vassbo, which were the largest lead producers in Europe during the second half of the 20th century. Hence, a number of publications are available for this mineralization system /e.g. Grip 1954, 1967, 1973, Tegengren 1962, Lilljequist 1973, Rickard et al. 1979, 1981, Christoffersson et al. 1979, Bjørlykke 1983, Bjørlykke and Sangster 1981, Bjørlykke and Thorpe 1982, Lindblom 1982, Kendrick et al. 2005/. The close affinity to Vendian or Early Cambrian sandstones, the mineralogical and isotopic compositions as well as the fluid inclusion characteristics of this mineralization type are very similar compared to the vein-hosted mineralizations and a genetic link between these two mineralization types has often been put forward.

The age and origin of the sandstone-hosted mineralization have, however, been difficult to asses and these topics have been in focus for considerable amounts of discussions. /Grip 1954/ and /Rickard et al. 1979/ were convinced about a Caledonian age for the Laisvall deposit and suggested long-transported hydrothermal fluids from the interior of the Caledonides. /Tegengren 1962/ concluded that both Caledonian and Permian ages were plausible alternatives for the timing of the Vassbo deposit, in particular noting the possible genetic link between sandstone-hosted lead, calcite-fluorite-galena veins near the Caledonian front, and calcite-fluorite-galena veins immediately associated with the Permian Oslo rift. /Bjørlykke and Sangster 1981/ assumed that all sandstone-hosted mineralizations in the Caledonian front had formed shortly after the deposition of the sediments. Furthermore, based on a lead isotope study of the Osen deposit, /Bjørlykke and Thorpe 1982/ argued strongly for a local metal derivation (the granitic basement) and subsequent Early Cambrian redeposition of metals into the Early Cambrian clastic sediments.

Current ideas on the Laisvall deposit /Kendrick et al. 2005/ are in support of the early theories proposed by /Grip 1954/ and /Rickard et al. 1979/, indicating Late Silurian fluid derivation from Precambrian crustal units within the continental margin of Baltica, and migration of metals to the Caledonian front in conjunction with the main Caledonian overthrusting. This is consistent with the observation of Pb (and U) mobilization from the Precambrian basement in the interior parts of the Caledonides at 420 Ma /Stuckless et al. 1982/ and recent Ar-Ar dating at c 425 Ma of K-feldspar overgrowths associated with mineralization in Laisvall /Kendrick et al. 2005/.

3 Background to the Sm-Nd isotope method for dating fluorite

Ca-bearing minerals, like fluorite and calcite, may carry ppm levels of REE including Sm and Nd, which substitute for Ca in the crystal lattice. More or less successful efforts to determine ages of fluorite by the Sm-Nd isochron method have been reported for Phanerozoic fluorite mineralizations /Galindo et al. 1994, Chesley et al. 1991, 1994, Menuge et al. 1997/. With this method, Sm and Nd in fluorite are isotopically analyzed for some 3–6 samples within a mineralized system, so that the $^{143}Nd/^{144}Nd$ ratio of each sample can be plotted vs. the $^{147}Sm/^{144}Nd$ ratio in a standard Sm-Nd isochron diagram. Ideally, all data points with the same age form a straight line, an isochron, whose slope corresponds to the age of the analyzed samples. An important prerequisite for a meaningful age calculation is that all samples have the same initial $^{143}Nd/^{144}Nd$ ratios.

4 Present investigation

For the present investigation, Sm-Nd isotopic systematics in vein fluorite and calcite (fracture infillings) as well as fluorite cement in sandstone was utilized, in an attempt to determine the age of the Phanerozoic hydrothermal fluorite-calcite-galena mineralization event(s) in the margins of the Fennoscandian Shield. The veins represent three geological settings in the Baltic Sea region; Götemar, in a 1,452 Ma granite in southeastern Sweden, Tindered, in 1,859 Ma sheared granites along the northeastern margin of the Trans-scandinavian Igneous Belt (TIB) complex in southeastern Sweden, and Lovisa, in the c 1,640 Ma Wiborg batholith in southeastern Finland. The fluorite cement occurs in Vendian sandstone at Laisvall in the Caledonian front, northern Sweden.

A number of potential source rocks to the fluorite mineralizations were also selected for this study, following the assumption that Sm-Nd isotopic systematics in the source may be related to that of the precipitates in such a way that well constrained isochrons could be constructed.

4.1 Characteristics of the target areas

In all selected target areas with vein fluorite, the host rocks to the mineralizations typically display intense vertical fracturing, often with a spacing in dm-m scale with mineralization on most fractures. The mineralizations in the Tindered and Lovisa areas are well-exposed in road cuts along more than a kilometre, and in the Götemar area, fluorite is best exposed in a several hundred metres long quarry. At each site, abundant mineralized fractures can be observed, which may be up to several tens of metres long. The Götemar and Lovisa areas are dominated by ENE-NE trending structures, whereas NNE-NE trending structures dominate in the Tindered area /Sundblad and Alm 2000, Alm and Sundblad 2002/. The observed intensity of mineralized fractures over large volumes of bedrock suggests that the Precambrian crust was subject to a large and sudden stress fields in conjunction with the hydrothermal activity.

4.1.1 Götemar area

The Götemar A-type granite intrusion has a diameter of five km and is located 30 km northeast of Oskarshamn (Figures 4-1, 4-2 and 4-3). This pluton is dominated by a coarse, even-grained granite containing around 0.35–0.40% F, sitting in fluorite as well as F-rich biotite /Kresten and Chyssler 1976, Alm and Sundblad 2002/. Subhorizontal fluorite- and topaz-bearing pegmatites are locally found within and outside the pluton /Kresten and Chyssler 1976/. Several age determinations employing different minerals and different methods have been carried out on the Götemar granite /Åberg et al. 1984, Smellie and Stuckless 1985, Åberg 1988/ but the best age estimate is 1,452 +11/–9 Ma, obtained by /Åhäll 2001/. Mm-dm-wide vertical Cambrian sandstone dykes are abundant in the eastern part of the pluton, particularly in the Kråkemåla 2 quarry. Fluorite veins are observed in many of the quarries in the Götemar granite, including Askaremåla, Kråkemåla 1 and 2, Bussvik, and Götebo. Fluorite veins are also found in the older TIB rocks immediately outside the Götemar pluton. /Kresten and Chyssler 1976/ paid particular attention to the fact that the dykes with Cambrian sandstone only were found east of the fault seen in Figure 4-2, and concluded a post-Cambrian age for this structure. The fault is of more than local importance, because it continues for at least 20 km towards the north /Kresten and Chyssler 1976, Lundegårdh et al. 1985/.

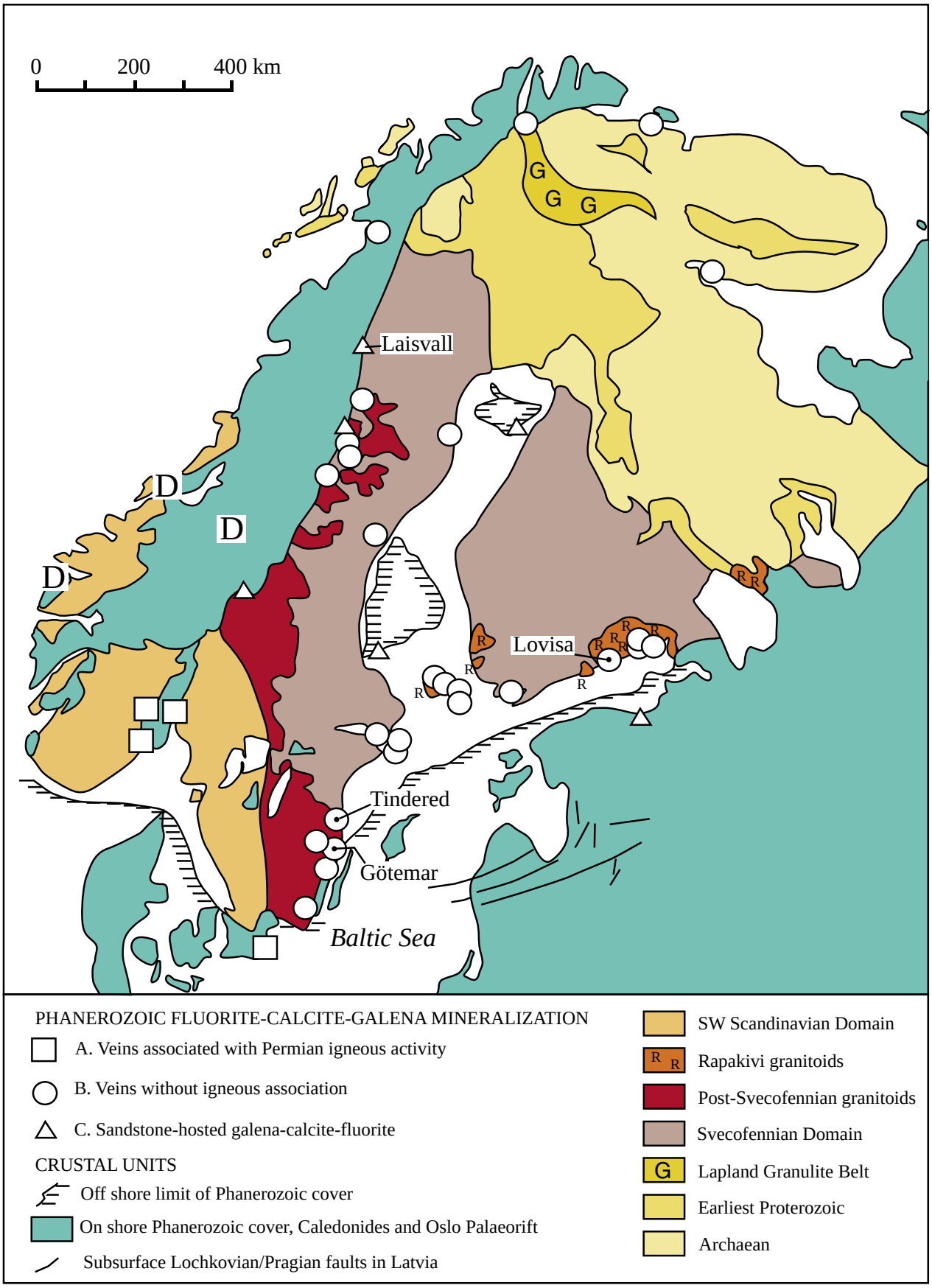

Figure 4-1. *Geology of the Fennoscandian Shield with location of the investigated areas and other relevant fluorite-calcite-galena mineralizations. D = Devonian sedimentary rocks in intermontane Caledonian basins.*

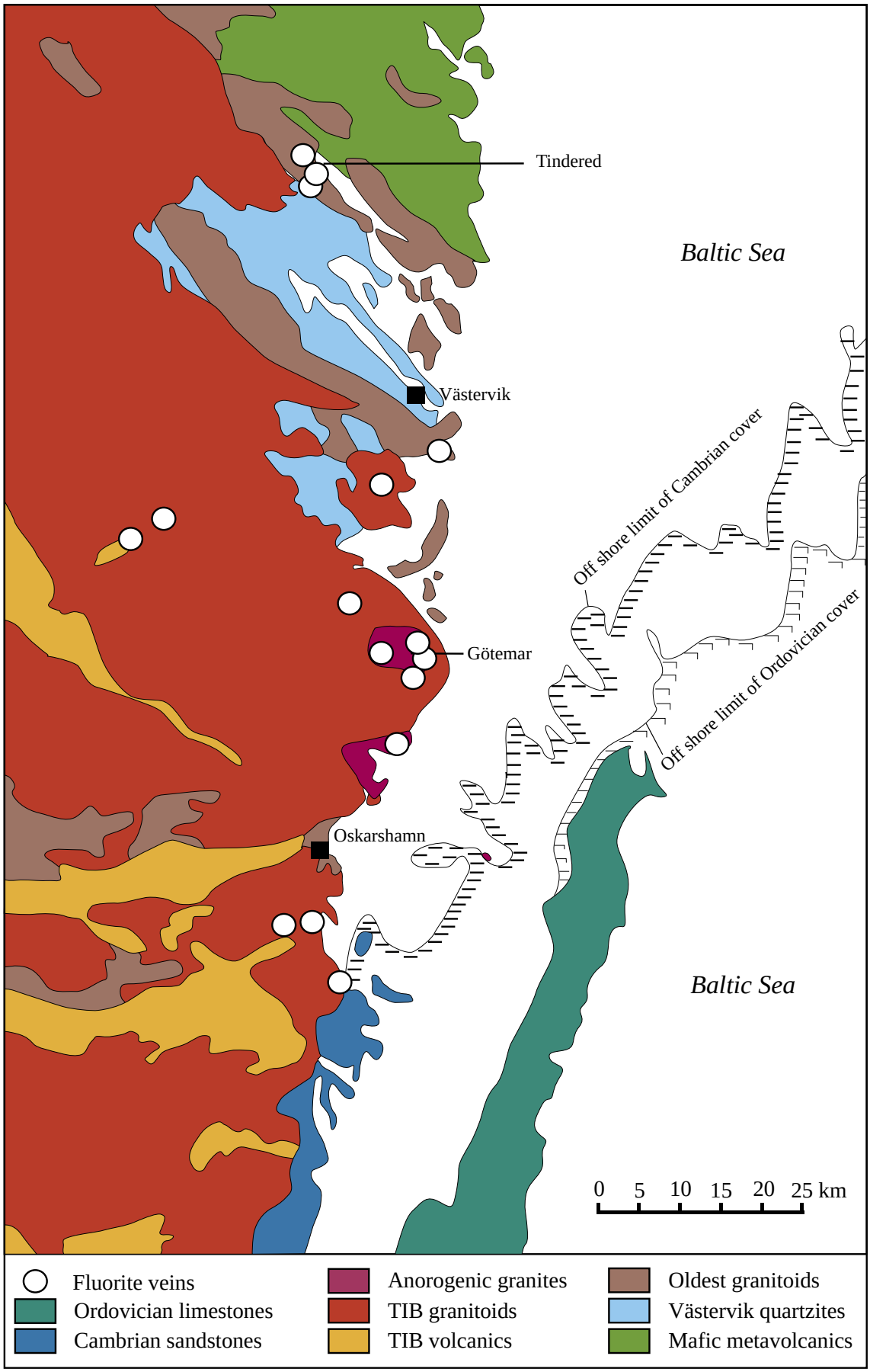

Figure 4-2. *Geology of the northern part of Kalmar county with location of Götemar and Tindered, and other fluorite-calcite-galena mineralizations.*

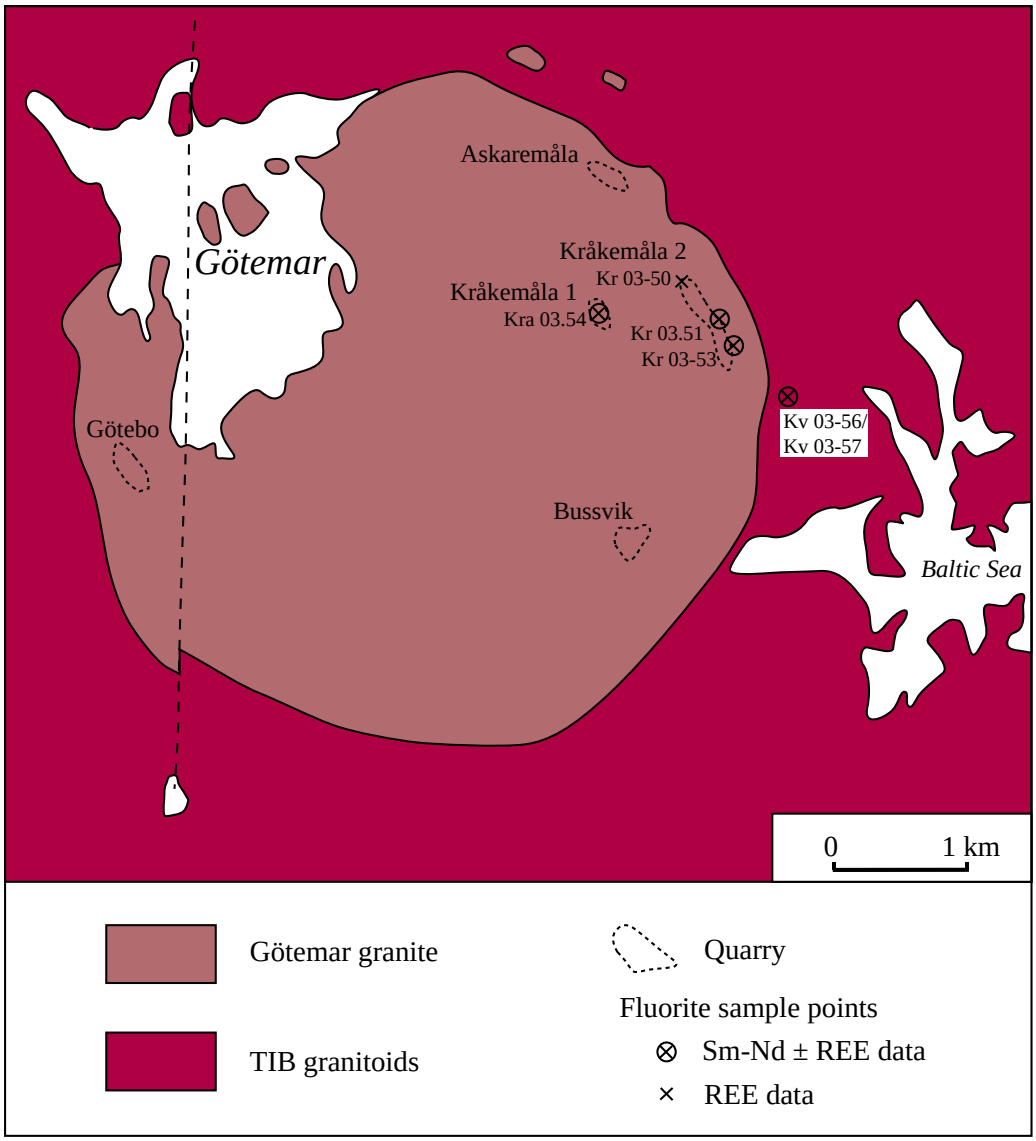

Figure 4-3. *Geology of the Götemar area /Kresten and Chyssler 1976/ with location of investigated samples.*

4.1.2 Tindered area

The 'Tindered granite' is an informal name for a characteristic rock unit occurring along the border between the TIB and the metamorphosed Svecofennian complex, some 30 km northwest of Västervik (Figures 4-1 and 4-2). This granite is in part strongly sheared, probably by movements in the Precambrian NW-trending Loftahammar-Linköping deformation zone (LLDZ; /Beunk and Page 2001/), which passes just north of Tindered. The granite was marked as "Older granite" and "Older granite and granodiorite, porphyritic" by /Lundegårdh et al. 1985/ on the regional 1:250,000 map sheet. Recent work on this unit has shown that it has an age of 1,859 Ma (H Wikman, SGU Lund, pers. comm. 2004) and that two main granite types can be distinguished: "biotite granite" and "porphyritic granite" /Alm and Sundblad 2002/. The geochemical signatures of these two rock types are indicative of metaluminous, differentiated granites. The F content in the biotite granite ranges from 0.22 to 0.25% and is slightly lower in the porphyritic granite (c 0.18%). Fluorite has been documented as accessory phase in both granites /Alm and Sundblad 2002/. Fluorite veins are abundant in the exposures along the main road (Figure 4-4) and one vein is associated with Cambrian sandstone dykes.

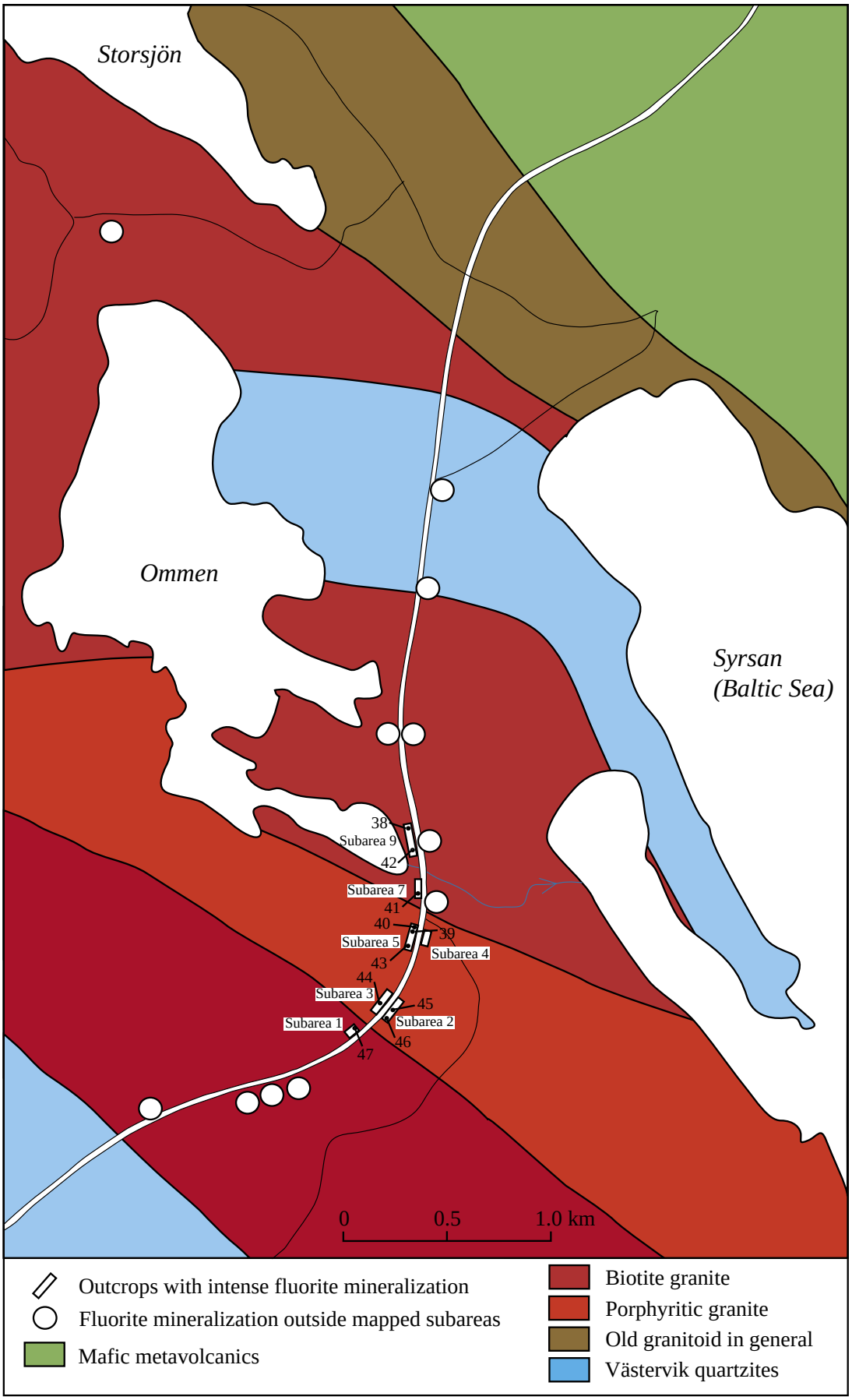

Figure 4-4. *Geology of the Tindered area /Alm and Sundblad 2002/ with location of investigated samples in short notation; see Table 5-1 for complete sample numbers.*

4.1.3 Lovisa area

The Wiborg batholith is located in southeastern Finland and in adjoining areas in Russia (Figure 4-1). It is the largest of the Fennoscandian rapakivi plutons and was emplaced from 1,650 Ma to 1,625 Ma /Vaasjoki et al. 1991/. The pluton consists of several rock types, including wiborgite (with spectacular mantled feldspars), pyterlite, coarse- and even-grained rapakivi as well as porphyry aplite. The chemical character of the rocks in the Wiborg batholith is typical for A-type granites and the high contents of F (c 0.5%) have often allowed for fluorite to form in the rock in addition to F-rich biotite /Alm and Sundblad 2002/. Vertical fractures with infillings of fluorite occur in the Lovisa area (Figure 4-5), where two subareas are identified: 1) Metsola, on the main road between Lovisa and Kotka, some 8–10 km east of Lovisa and 2) Hästholmsvägen, some 3 km southeast of Lovisa, on the road connecting Lovisa with the nuclear power plant at Hästholmen. These sites are located on the map sheets 3023 Kotka and 3021 Porvoo but were not recognized when /Laitala 1964/ and /Simonen and Laitala 1970/ published their respective bedrock map. The Metsola fluorites are located in a (fault-controlled?) sliver of pyterlite, only few hundred metres from surrounding varieties of wiborgite and some 1–2 km east of an even-grained rapakivi granite. The Hästholmsvägen fluorites are located on the border between a wiborgite and a porphyry aplite.

4.1.4 Laisvall area

The sandstone-hosted galena-fluorite deposit at Laisvall is located in the Caledonian front in northern Sweden and was the largest lead producer in Europe for many years during the latter part of the 20th century. At Laisvall, galena, fluorite, calcite and barite act as cementing agents in Vendian and Lower Cambrian sandstones /Grip 1954/. Local variations in the proportions of these minerals are recorded. Galena dominates in the central parts of the mineralized area, whereas the other cementing agents surrounds the galena ore /Carlsson 1970/. A small but intense fluorite-galena mineralization occurs at Ackerselet, some 20 kilometres south of the mine. This mineralization is found in the Ackerselet Formation, which constitutes the lowermost unit of the sedimentary sequence at Laisvall /Willdén 1980/. It is underlain by granite and syenite /Lilljequist 1973/ that belongs to the c 1,790 Ma /Skiöld 1988/ Sorsele suite.

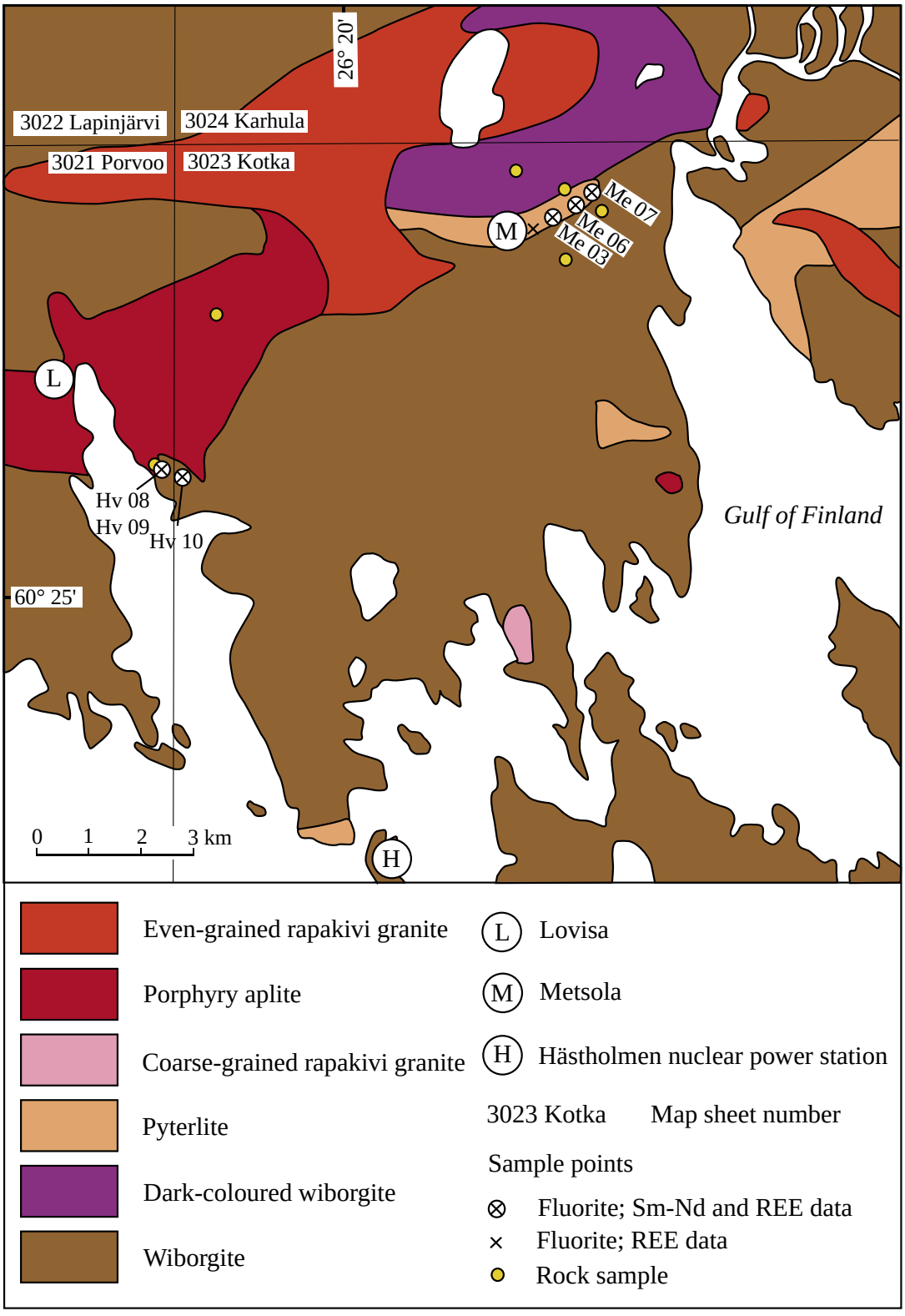

Figure 4-5. *Geology of the Lovisa area /Laitala 1964, Simonen and Laitala 1970, Laitakari and Simonen 1962, Simonen 1965/ with location of investigated samples in short notation; see Tables 5-1 and 5-2 for complete sample numbers.*

5 Description of samples

5.1 Fluorite and calcite from fracture infillings

The investigated vein fluorite and calcite is typically found as thin coatings on fracture planes, which have become exposed when roads (or quarries) were constructed/exploited. Fluorite and calcite veins outside these artificial outcrops are very rare. The general appearance of the fluorite is quite similar in all three target areas, despite their wide geographical distribution. Most fluorites exhibit intergrown, well developed cubic crystal faces on the surface (centre of fracture during formation). However, crystal size and colour varies, even within individual fracture planes in each area. Only in one fracture at Tindered, a weak colour banding was observed (see below). No field evidence argues against a contemporaneous formation of the fluorite fracture infillings within each of the three investigated areas. Fluorite (and calcite) samples from thin (< 10 mm), vertical-subvertical fracture infillings were collected from six sites in the Götemar area (Figure 4-3), ten sites in the Tindered area (Figure 4-4), and ten sites in the Lovisa area (Figure 4-5). At one site in Götemar and at one site in Tindered, abundant calcite is intergrown with the fluorite and coprecipitated mineral pairs could thus be separated for isotope analysis. All samples are listed in Table 5-1.

In the *Götemar* area, fluorite was collected in the abandoned Kråkemåla 2 quarry (Kr 03-50, Kr 03-51, Kr 03-53), in the active Kråkemåla 1 quarry (Kra 03-54), and in a road cut southeast of Kråkemåla 2 (Kv 03-56, Kv 03-57), see Figure 4-3. All Kråkemåla fluorites are hosted in coarse-grained Götemar granite. The two samples (# 56 and # 57) from the road cut are hosted in a fine-grained Småland granite, which is partly sheared near the contact to the Götemar granite. Of the three Kråkemåla 2 samples, # 50 was taken from a thin, very fine-grained, dark purple fluorite-coating on a large dimension stone. Under the microscope, this fracture infilling proved to be greisen-like, consisting of extremely fine-grained fluorite, like a fine powder, and considerable amounts of white mica. This fluorite is considered not to be related to the Phanerozoic mineralizing event but more likely to a late magmatic stage of the Götemar intrusion. It is therefore not included in the isotope study. Sample # 51 was taken in a fracture, which crosscuts a sandstone dyke (close to field obs. 89:18 in /Alm and Sundblad 2002/) and consists of mm-sized crystals of purple fluorite associated with calcite. Sample # 53 is from a fracture plane with a sandstone dyke and fluorite coating on the sandstone (field obs. 89:16 in /Alm and Sundblad 2002/). The fluorite crystals are less than 1 mm in size, clear and colourless or purple. The Kråkemåla 1 sample consists of mm-sized purple fluorite grains associated with some calcite. The fluorite in # 56 (from the same fracture plane as sample GM 01-15 in /Alm and Sundblad 2002/) and # 57 (some 70 m to the north) is yellow to colourless or pale purple, with up to 1 cm-sized crystals. Pyrite is common on the fracture where sample # 56 was collected. Very few and small solid inclusions were seen in the fluorites sampled in the Götemar area.

The *Tindered* fluorites were sampled in subareas 1, 2, 3, 5, 7 and 9 /Alm and Sundblad 2002/ in both types of granitic host rocks (Figure 4-4). The fluorite crystals are commonly up to 0.5 mm or rarely 10 mm in size. The colour varies from very dark purple (one specific site in subarea 9; sample Ti 03-38) to semibanded bluegreen-pale purple (one specific site in subarea 5; sample Ti 03-44; same as Ti 01-18 in /Alm and Sundblad 2002/, pale purple, yellow or white/colourless. Calcite and galena are associated with fluorite in sample # 44. Galena is also present in samples # 40, 41, and 45. Only two of the fluorite samples (# 45 and 46) contain solid inclusions. These are probably amorphous Fe-hydroxide, undetectable with X-ray diffraction.

Table 5-1. Mineral samples.

Sample #	Mineral	Area	Site	E/N Coordinates*	Host rock	Analysis
Kr 03-50	fluorite	Götemar	Kråkemåla 2	1550384/6373105	Götemar granite	REE
Kr 03-51	fluorite	Götemar	Kråkemåla 2	1550673/6372752	Götemar granite	Sm-Nd
Kr 03-51a	calcite	Götemar	Kråkemåla 2	1550673/6372752	Götemar granite	Sm-Nd
Kr 03-53	fluorite	Götemar	Kråkemåla 2	1550799/6372614	Götemar granite/ss dyke	Sm-Nd
Kra 03-54	fluorite	Götemar	Kråkemåla 1	1549769/6372963	Götemar granite	REE, Sm-Nd
Kv 03-56	fluorite	Götemar	SE of Kråkemåla	1551204/6372360	TIB granitoid, contact zone	REE, Sm-Nd
Kv 03-57	fluorite	Götemar	SE of Kråkemåla	1551242/6372433	TIB granitoid, contact zone	REE, Sm-Nd
Ti 03-38	fluorite	Tindered	Subarea 9	1540147/6428521	biotite granite	REE, Sm-Nd
Ti 03-39	fluorite	Tindered	Subarea 5	1540157/6428041	porphyritic granite	REE, Sm-Nd
Ti 03-40	fluorite	Tindered	Subarea 5	1540158/6428048	porphyritic granite	REE, Sm-Nd
Ti 03-41	fluorite	Tindered	Subarea 7	1540182/6428224	biotite granite	REE, Sm-Nd
Ti 03-42	fluorite	Tindered	Subarea 9	1540163/6428454	biotite granite	REE, Sm-Nd
Ti 03-43	fluorite	Tindered	Subarea 5	1540124/6427942	porphyritic granite	REE, Sm-Nd
Ti 03-44	fluorite	Tindered	Subarea 3	1539946/6427666	porphyritic granite	REE, Sm-Nd
Ti 03-44B	calcite	Tindered	Subarea 3	1539946/6427666	porphyritic granite	Sm-Nd
Ti 03-45	fluorite	Tindered	Subarea 2	1539983/6427668	porphyritic granite	REE, Sm-Nd
Ti 03-46	fluorite	Tindered	Subarea 2	1539957/6427640	porphyritic granite	REE, Sm-Nd
Ti 03-47	fluorite	Tindered	Subarea 1	1539856/6427570	biotite granite	REE, Sm-Nd
Me 03-01	fluorite	Lovisa	Metsola	3466920/6708290	pyterlite	REE
Me 03-02	fluorite	Lovisa	Metsola	3467000/6708280	pyterlite	REE
Me 03-03	fluorite	Lovisa	Metsola	3467270/6708440	pyterlite	REE, Sm-Nd
Me 03-04	fluorite	Lovisa	Metsola	3467290/6708450	pyterlite	REE
Me 03-05	fluorite	Lovisa	Metsola	3467330/6708460	pyterlite	REE
Me 03-06	fluorite	Lovisa	Metsola	3467660/6708600	pyterlite	REE, Sm-Nd
Me 03-07	fluorite	Lovisa	Metsola	3467780/6708660	pyterlite	REE, Sm-Nd
Hv 03-08	fluorite	Lovisa	Hästholmsvägen	3459800/6703570	porphyry aplite	REE, Sm-Nd
Hv 03-09	fluorite	Lovisa	Hästholmsvägen	3459770/6703570?	porphyry aplite	REE, Sm-Nd
Hv 03-10	fluorite	Lovisa	Hästholmsvägen	3460120/6703380	wiborgite	REE, Sm-Nd
Ak 2:1	fluorite	Laisvall	Ackerselet Ddh 2, 7.57–8.30 m	1563028/7321248	Vendian sandstone	Sm-Nd
Ak 4:1	fluorite	Laisvall	Ackerselet Ddh 4, 5.13–6.01 m	1563020/7321180	Vendian sandstone	Sm-Nd
Ak 5:1	fluorite	Laisvall	Ackerselet Ddh 5, 13.71–13.73 m	1563084/7321180	Vendian sandstone	Sm-Nd
Ak 5:2	fluorite	Laisvall	Ackerselet Ddh 5, 15.20–15.29 m	1563084/7321180	Vendian sandstone	Sm-Nd
Ak 6:1	fluorite	Laisvall	Ackerselet Ddh 6, 13.69–14.02 m	1563096/7321232	Vendian sandstone	Sm-Nd

*Swedish and Finnish national grids respectively.

ss = sandstone; Ddh = diamond drillhole.

Of the ten *Lovisa* fluorites, seven were collected in road cuts located along c one km of the main road east of Metsola (samples Me 03-01 to 03-07), see Figure 4-5. The colour of the fluorite is mostly yellow, white/colourless or to a lesser extent pale purple. The fluorite is fairly coarse-grained and crystals 0.5–1 cm in size are abundant. The host rock is a pyterlite. Three fluorites were sampled in two road cuts along Hästholmsvägen; samples Hv 03-08 and Hv 03-09 in two outcrops on either side of the road c 3 km southeast of Lovisa, and Hv 03-10 c 450 m further to the southwest. The fluorite is similar at all sites; pale yellow or purple to white/colourless, with crystals up to 0.5 cm in size. The host rock to sample # 10 is a wiborgite, while # 08 and 09 are hosted in a porphyric aplite. It can be noted that no calcite or galena is found associated with the fluorite in the observed outcrops in the Lovisa area. Calcite and dolomite together with fluorite is, however, reported by /Gehör et al. 1997/ in fracture infillings in the Wiborg batholith, observed in drillcores at the site for the nuclear power plant at Hästholmen. Most of the fluorites from the Lovisa area contain solid inclusions, probably amorphous Fe-hydroxide as in the Tindered area.

5.2 Fluorite as cement in sandstone

Five fluorite-rich sections in four drillcores from *Ackerselet* were selected (Table 5-1). Pale purple fluorite fills the pore space between fairly rounded but poorly sorted detrital grains, mainly quartz with minor feldspar. The grain size of the light grey sandstone is approximately in the range 0.1–10 mm. Small amounts of Fe sulphides and barite (?) accompanies the fluorite, whereas visible galena impregnation mostly is found a few metres higher up in the sections. The sub- to anhedral fluorite crystals are clear without solid inclusions and the grain size is ≤ 2 mm.

5.3 Potential source rocks to fluorite mineralizations

All rock samples are listed in Table 5-2. One sample each of the two granite types at Tindered was collected in the road cuts (Figure 4-4). Of the coarse-grained, dark red Götemar granite, one sample was taken in the active quarry (Kråkemåla 1) and one in the abandoned (Kråkemåla 2; Figure 4-3). In the Lovisa area, two pyterlite samples were collected in the Metsola road cuts, dark wiborgite in natural outcrops at two sites, north and northeast of Metsola, two wiborgite samples in natural outcrops south and southeast of Metsola and one in the northwestern road cut at Hästholmsvägen. Porphyry aplite was sampled in the same road cut at Hästholmsvägen and at Tessjö, in a small road cut along the main road between Lovisa and Metsola (Figure 4-5). Fresh and representative samples of the Sorsele suite underlying the Ackerselet fluorite mineralization were collected from two drillcores.

Table 5-2. Rock samples.

Sample #	Area	Site	E/N Coordinates*	Rock type	Analysis
Kr 0417	Götemar	Kråkemåla 1	1549810/6372850	Götemar granite	Chem, Sm-Nd
Kr 0418	Götemar	Kråkemåla 2	1550660/6372745	Götemar granite	Chem, Sm-Nd
Ti 0419	Tindered	Subarea 5	1540157/6428052	porphyritic granite	Chem, Sm-Nd
Ti 0420	Tindered	Subarea 9	1540160/6428448	biotite granite	Chem, Sm-Nd
Me 0401	Lovisa	Metsola	3466950/6708250	pyterlite	Chem, Sm-Nd
Me 0402	Lovisa	Metsola	3467360/6708450	pyterlite	Chem
Me 0403	Lovisa	Metsola	3467530/6709110	dark wiborgite	Chem, Sm-Nd
Me 0408	Lovisa	Metsola	3466640/6709450	dark wiborgite	Chem, Sm-Nd
Me 0404	Lovisa	Metsola	3468270/6708700	wiborgite	Chem
Me 0409	Lovisa	Metsola	3467580/6707750	wiborgite	Chem
Hv 0405	Lovisa	Hästholmsvägen	3459760/6703600	wiborgite	Chem, Sm-Nd
Hv 0406	Lovisa	Hästholmsvägen	3459800/6703570	porphyry aplite	Chem, Sm-Nd
Te 0407	Lovisa	Tessjö/Tessjoki	3460810/6706680	porphyry aplite	Chem, Sm-Nd
Ak 0415	Laisvall	Ackerselet Ddh 24, 94.27–94.68 m	1564120/7322890	Sorsele granite	Chem, Sm-Nd
Ak 0421	Laisvall	Ackerselet Ddh 4, 14.16–14.68 m	1563020/7321180	Sorsele granite	Chem, Sm-Nd

*Swedish and Finnish national grids respectively.

6 Analytical methods

Fluorite was mechanically separated from adjacent wall rock fragments and 3–10 g of fluorite grains were handpicked in alcohol under microscope and ground in an agate mortar. Varying (but mostly small) amounts of included Fe-hydroxide, pyrite (marcasite?), or calcite could not be avoided in these separates. The 15 rock samples were crushed and milled. Four Götemar, ten Tindered, and ten Lovisa fluorite separates were analyzed for trace element contents and the rock powders for major and trace element contents using ICP-MS at Acme Analytical Laboratories LTD, Vancouver. The F content in the rock powders was determined at the Laboratory of Geological Survey of Estonia, Tallinn, using ion-selective electrode.

Six fluorite samples from the Lovisa and Götemar areas respectively, and all Tindered and Laisvall mineral samples, were selected for the isotopic investigation, partly based on the results of the ICP-MS analyses. Some 150 mg of purest possible fluorite and calcite grains were handpicked in alcohol under microscope. 18–150 mg of the fluorites were dissolved on hot plate in Savillex screw-cap Teflon beakers using HCl and H_3BO_3. The calcites were dissolved in HCl and the rock powders in Teflon bombs in oven. Standard procedures /e.g. Hanski et al. 2001/ were used for chemical treatment and mass-spectrometry. Chemistry and isotope analyses (VG sector 54 MS) were conducted at the Geological Survey of Finland, Espoo. Age calculations were performed using Isoplot/Ex rev. 2.49 /Ludwig 2001/.

7 Results

a. Geochemistry of potential source rocks

The geochemical composition of the sampled rocks is given in the Appendix. Most rocks in this study plot in the granite field in the SiO_2 vs. Na_2O+K_2O discrimination diagram by /Cox et al. 1979/. An exception is the dark wiborgite Me 0403, which falls in the quartz diorite field. In a PQ diagram /Debon and Le Fort 1982/ the same dark wiborgite plots in the adamellite (monzogranite) field, together with the pyterlite Me 0409, the Götemar granite Kr 0417, the Tindered biotite granite Ti 0420, and the Sorsele granite Ak 0421. All others plot as true granites.

Chondrite-normalized /Boynton 1984/ REE profiles for rocks analyzed in the present study are presented in Figure 7-1a–d. For the Tindered and Götemar granites, previously published data /Alm and Sundblad 2002, Wikman and Kornfält 1995/ are included. All Götemar granites have highly fractionated LREE and the majority show a HREE pattern with a characteristic curve, dipping from Gd to Dy or Ho and then rising to Lu. Negative Eu-anomalies are generally present but of highly variable size. In the LREE a minor but clear division into two groups with different total REE contents can be noted. The Tindered granites show a fractionated LREE and fairly flat HREE pattern, with negative Eu-anomalies that are larger for the more evolved biotite granite than for the porphyritic granite. The biotite granite also has slightly higher LREE contents. A similar pattern, with fractionated LREE and fairly flat HREE, is displayed by the various Wiborg rapakivi granites. A distinct separation into two groups is obvious in that pyterlites and porphyry aplites have higher LREE contents and much larger negative Eu-anomalies than the wiborgites. The Sorsele granites from Ackerselet show only slight fractionation in all REE, with a small negative Eu-anomaly, indicative of a less evolved magma source compared to the other granites in this study.

b. Geochemistry of fluorites

The results of the trace element analyses of fluorites are presented in Table 7-1 and plotted in Figure 7-2a–c, presenting chondrite-normalized REE profiles.

For the Götemar area, REE data are available for four fluorite samples, of which only one is from a typical fluorite vein within the Götemar granite (Kra 03-54). The other three are the greisen-like fluorite (Kr 03-50) and the two fluorite samples collected immediately outside the Götemar granite (Kv 03-56, Kv 03-57). Two of the other Götemar samples were too small to allow for REE analyses. Sample Kra 03-54 displays a slightly fractionated LREE pattern, a pronounced negative Eu anomaly and fairly flat HREE but with some enrichment in the MREE. The REE pattern for the greisen-like sample (Kr 03-50) shows more fractionated LREE, a smaller Eu anomaly and lower HREE content compared to # 54. The REE patterns of samples # 56 and 57 are similar to each other but differ from that of # 54 through lower LREE content, flat LREE, smaller Eu anomalies, and fairly flat HREE that are significantly enriched relative to the LREE.

Ten data sets are available for the REE contents in Tindered fluorites. Eight of these have fairly uniform REE patterns, with rather flat LREE curves, pronounced negative Eu anomalies, and HREE that are constantly enriched relative to the LREE, although slightly decreasing from Er to Lu. Ti 03-41 has a similar pattern but generally with higher total REE contents. Ti 03-44 (the only sample consisting of green fluorite) is significantly more fractionated both in LREE and HREE, displaying a marked relative HREE depletion, and the smallest Eu-anomaly among the Tindered fluorites.

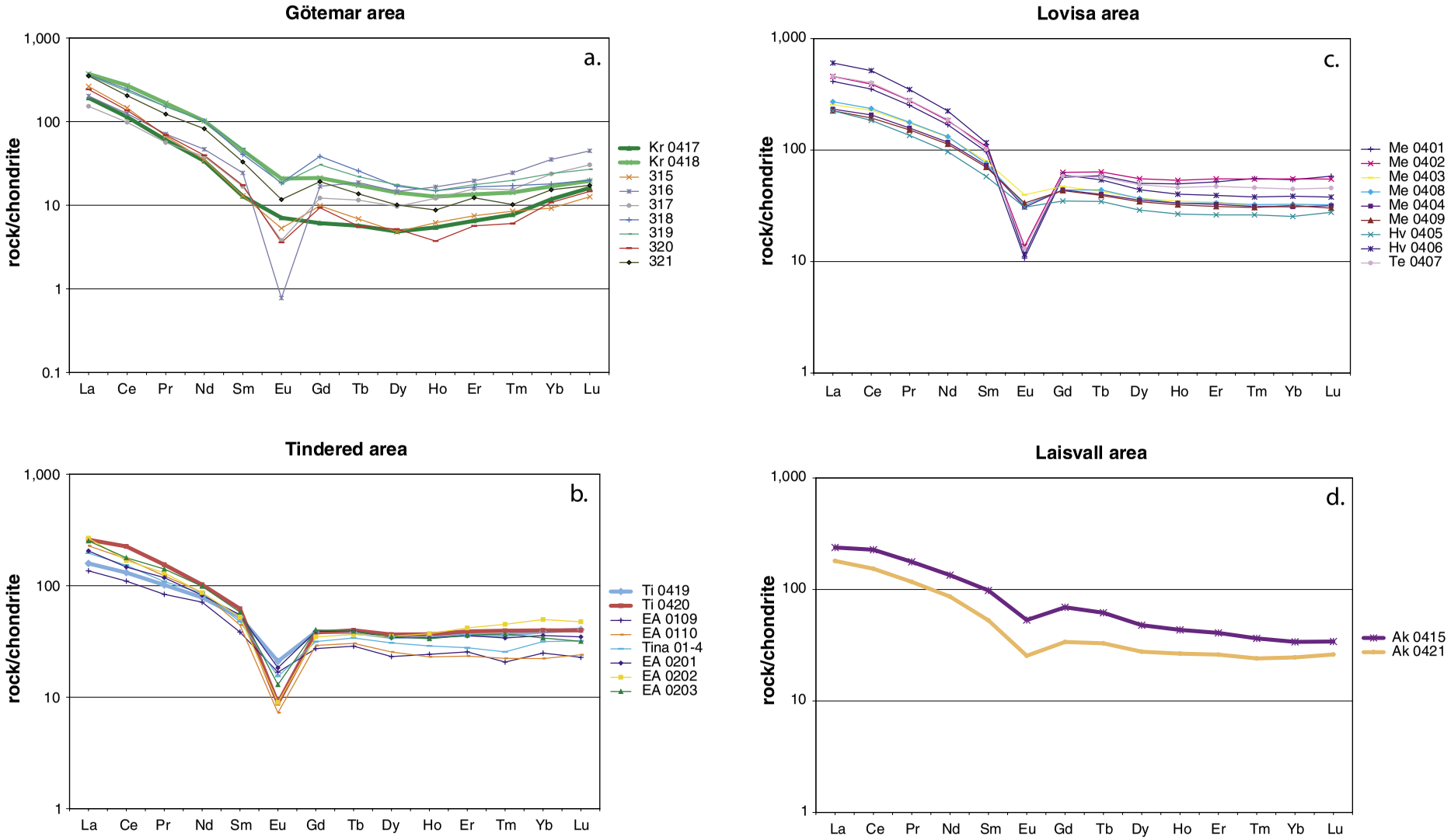

Figure 7-1. *REE patterns for a) the Götemar granite (# 315–321 from /Wikman and Kornfält 1995/); b) the Tindered granites (curves shown with thin lines from /Alm and Sundblad 2002/); c) the Wiborg batholith in the Lovisa area; d) the basement granite to the Ackerselet deposit in the Laisvall area.*

Table 7-1. Trace element content (ppm) in fluorite.

	Götemar				Tindered									
	Kr 03-50	Kra 03-54	Kv 03-56	Kv 03-57	Ti 03-38	Ti 03-39	Ti 03-40	Ti 03-41	Ti 03-42	Ti 03-43	Ti 03-44	Ti 03-45	Ti 03-46	Ti 03-47
Co	1.0	3.8	2.5	2.3	5.3	1.5	1.8	1.7	38.5	1.5	1.1	31.6	39.1	1.5
Sr	53.4	41.0	64.3	90.1	37.3	54.8	43.7	60.4	43.8	40.4	82.4	64.8	69.2	65.7
Th	4.9	3.2	0.4	1.2	1.0	0.2	0.5	0.2	0.8	0.4	0.1	<0.1	0.4	0.4
U	8.6	21.1	<0.1	0.3	0.5	0.1	1.5	0.3	0.3	<0.1	0.2	0.2	4.0	0.4
W	0.7	0.4	0.4	0.4	0.2	0.5	0.7	0.4	0.4	0.4	0.3	0.4	0.4	0.4
Zr	21.5	12.4	0.5	1.5	0.9	0.7	1.0	<0.5	0.7	1.3	<0.5	1.1	2.2	0.7
Y	147.1	338.7	430.0	663.5	365.4	347.7	407.2	1189.7	442.1	429.6	718.6	432.2	470.6	415.2
La	18.5	21.9	9.0	12.3	13.8	7.6	15.3	23.3	9.7	10.5	25.7	8.4	8.0	11.9
Ce	35.8	49.1	23.9	32.7	33.2	19.3	34.8	59.8	22.6	24.5	78.7	23.1	21.0	32.6
Pr	3.39	5.28	3.20	4.48	4.02	2.75	4.66	9.07	3.06	3.39	15.33	3.34	3.04	4.15
Nd	13.0	21.5	17.0	22.8	18.2	15.6	22.7	48.2	14.0	15.7	104.6	17.1	15.0	19.9
Sm	3.9	7.0	6.5	9.6	7.6	7.5	9.1	31.1	6.2	8.9	56.8	7.9	7.2	7.1
Eu	1.03	1.24	1.62	2.31	0.99	1.13	1.21	4.70	0.82	1.33	11.09	1.33	1.31	1.03
Gd	7.67	10.53	13.21	17.77	13.25	14.18	16.33	57.28	13.10	16.63	92.09	15.52	13.62	12.94
Tb	1.59	2.51	3.57	4.99	3.49	3.57	4.18	17.52	3.95	4.90	16.89	4.07	4.06	3.44
Dy	8.52	14.16	21.11	31.00	23.04	20.68	24.25	105.16	25.24	28.65	70.51	24.79	26.06	20.38
Ho	1.93	3.67	4.86	7.16	5.74	4.72	5.88	24.44	6.49	6.81	12.56	5.80	6.26	5.28
Er	5.19	11.74	15.41	22.97	17.92	12.74	17.29	76.98	20.28	20.15	26.72	16.47	18.17	16.44
Tm	0.74	1.76	2.19	3.31	2.32	1.73	2.33	11.32	2.86	2.70	2.32	2.14	2.40	2.29
Yb	3.72	11.21	12.32	18.78	13.07	9.02	13.59	65.23	17.13	14.66	8.84	11.62	12.60	13.72
Lu	0.58	1.98	1.92	2.85	1.83	1.24	1.85	9.15	2.35	1.99	1.35	1.52	1.65	1.75

Table 7-1. Continued.

	Lovisa									
	Me 03-01	Me 03-02*	Me 03-03	Me 03-04	Me 03-05	Me 03-06	Me 03-07	Hv 03-08	Hv 03-09	Hv 03-10
Co	10.8	4.2	14.0	23.1	1.7	3.0	12.6	8.3	2.8	6.0
Sr	73.2	67.5	86.5	69.8	77.1	82.7	71.3	70.5	70.5	117.0
Th	2.1	0.6	0.6	0.9	3.3	0.9	0.6	0.8	2.4	0.2
U	12.0	10.2	0.6	1.3	6.6	1.0	1.0	5.4	43.3	0.3
W	2.0	1.3	0.9	0.8	0.8	2.0	0.5	0.8	0.5	0.6
Zr	3.3	1.2	0.6	1.2	8.1	2.3	0.9	1.3	5.5	<0.5
Y	912.7	763.0	723.0	835.9	808.5	698.2	688.7	782.3	545.5	626.2
La	23.9	17.0	11.3	10.6	17.8	17.4	10.0	8.5	9.2	5.0
Ce	49.8	38.4	27.7	27.6	38.8	40.7	26.9	23.6	29.8	15.6
Pr	5.30	4.46	3.69	3.61	4.80	4.96	3.48	3.23	3.78	2.43
Nd	23.0	19.8	17.2	18.5	21.0	21.3	16.1	16.2	19.3	12.4
Sm	9.6	8.0	9.2	10.1	9.9	8.3	7.8	9.0	8.7	5.8
Eu	0.57	0.38	1.01	0.91	0.65	0.58	0.61	0.69	0.43	0.83
Gd	22.88	18.19	23.21	24.14	23.59	17.08	18.24	20.48	16.58	13.53
Tb	7.57	6.05	7.18	7.73	7.42	5.47	6.05	6.68	5.07	4.92
Dy	45.59	37.21	40.33	44.44	43.20	32.85	36.69	40.65	31.09	32.59
Ho	9.91	8.22	8.11	9.27	9.07	7.39	7.76	8.97	6.65	7.40
Er	27.14	22.33	21.17	23.92	23.66	19.19	20.87	23.94	18.46	21.06
Tm	3.22	2.64	2.47	2.72	2.65	2.35	2.53	2.97	2.25	2.61
Yb	14.75	12.38	11.23	12.66	11.83	11.34	11.53	13.60	11.50	12.46
Lu	1.84	1.50	1.33	1.41	1.22	1.31	1.35	1.70	1.42	1.57

*Average of two analyses.

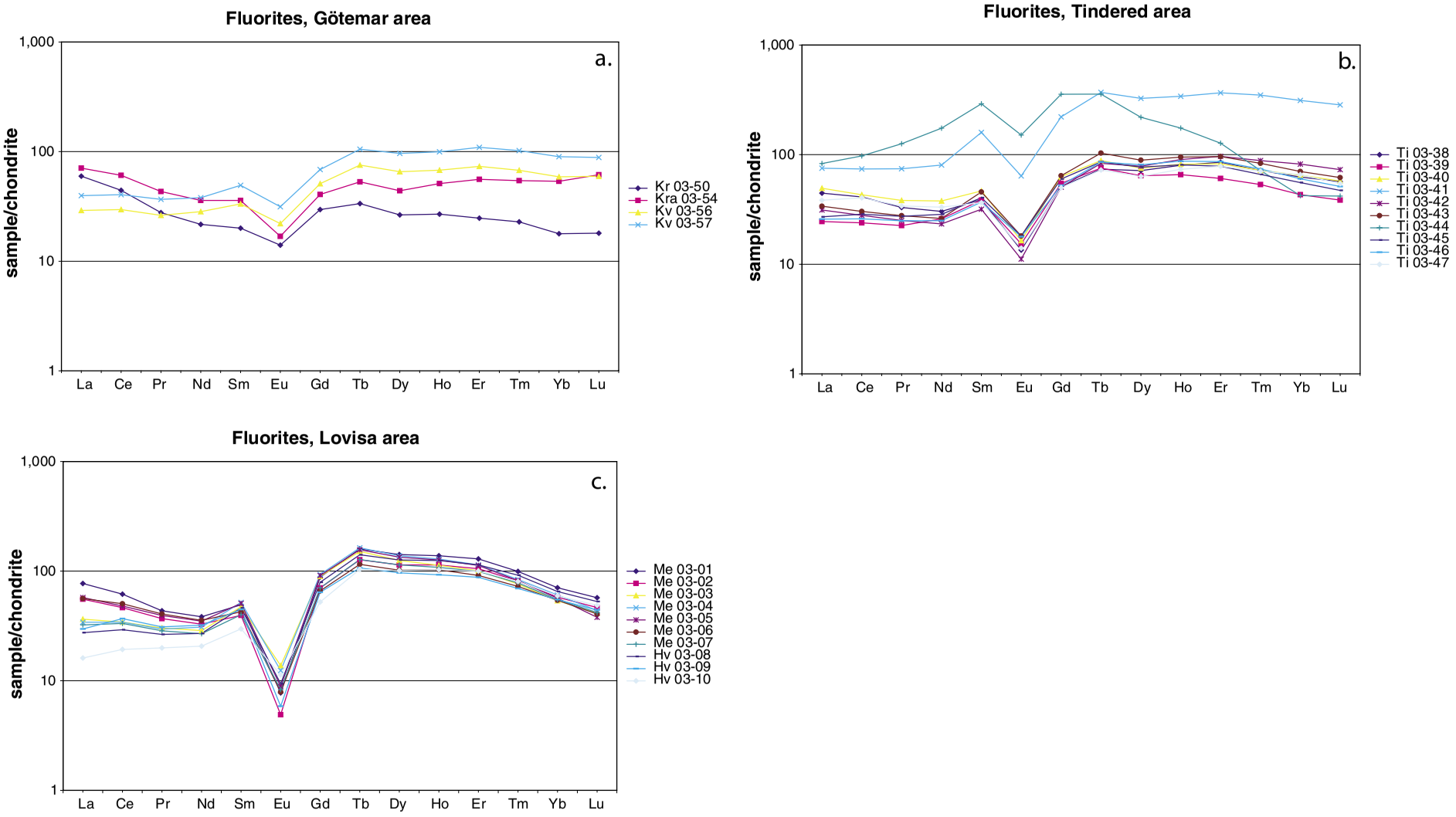

Figure 7-2. *REE patterns for a) the Götemar fluorites; b) the Tindered fluorites; c) the Lovisa fluorites.*

All ten REE profiles for Lovisa fluorites are similar, but display some variation in LREE fractionation. A weak distinction between the Metsola and Hästholmsvägen populations may be discerned. The latter (Hv 03-08 to 03-10) are slightly depleted in La relative to Ce, whereas the Metsola fluorites have flat LREE patterns or are enriched in La and Ce relative to Nd. For all samples, the negative Eu anomalies are large and HREE are enriched relative to the LREE but decreasing from Er to Lu (cf. Tindered profiles).

According to the ICP-MS data, the Sm and Nd contents of fluorite in the Götemar, Tindered and Lovisa areas are fairly high and display a narrow range (4 to 10 ppm Sm, and 12 to 23 ppm Nd) for most samples. The only exceptions are samples Ti 03-41 and Ti 03-44 (Tindered), which have distinctly higher contents (Figure 7-2b). The Sm/Nd ratios vary from 0.33 to 0.42 for the three non-greisen-like Götemar fluorites, from 0.36 to 0.65 for the Tindered fluorites, and from 0.39 to 0.56 for the Lovisa fluorites.

It can be noted that a weak tendency toward population-related elevations in other trace elements than REE exists, e.g. for Co in Tindered and Metsola, and for Th, U, W, and Zr in Kråkemåla and the Lovisa area. This observation is, however, not further discussed in the present study.

c. Sm-Nd isotopes

All Sm-Nd isotope analyses are technically of a high quality and the results are presented in Table 7-2 and Figures 7-3 to 7-8. The total concentration of Nd and Sm in fluorite from all study areas ranges from 8 to 26 ppm and from 2 to 10 ppm respectively. Two of the Tindered fluorite samples (# 41 and # 44) have distinctly higher concentrations of up to 117 ppm of Nd. These results are in agreement with the results obtained from the ICP-MS analyses. The two calcite samples have Nd concentrations of 54 and 117 ppm and low $^{147}Sm/^{144}Nd$ ratios compared to fluorite.

None of the obtained mineral data populations yield proper isochrons because of large MSWD values, indicating scatter much in excess of the analytical error. The reason for this scatter is probably a variation in initial $^{143}Nd/^{144}Nd$ ratios between samples. However, for each study area reference lines can be constructed, which provide age estimates that form a base for further elaboration on the timing of the hydrothermal vein formation. The fluorite-calcite pairs from the Götemar and Tindered areas contribute successfully to better constrain the age estimates. It is, on the other hand, clear that the isotope data from the suggested source rocks do not help in assessment of the fluorite ages.

Lovisa area

A reference line, including all the six analyzed fluorites from the Lovisa area (Figure 7-3), can be constructed, which corresponds to an age of 407 ± 54 Ma (MSWD = 5.0). The six rock samples, representing four different granite types within the Wiborg batholith, plot on a steeper line corresponding to an age of 1,565 ± 240 Ma (MSWD = 2.1). This age reflects within error limits the true intrusion ages of 1,650 to 1,625 Ma (as established by U-Pb chronology on zircons; /Vaasjoki et al. 1991/).

Table 7-2. Sm-Nd isotope data.

Sample/anal#	Location	Sample type	Sm (ppm)	Nd (ppm)	$^{147}Sm/^{144}Nd$	$^{143}Nd/^{144}Nd$	eNd (420)
Götemar area							
Kr 03-51 fl	Kråkemåla 2	Fluorite	9.16	25.62	0.2161	0.511901	–15.5
Kr 03-51a	Kråkemåla 2	Calcite	7.12	44.16	0.0975	0.511562	–15.7
Kr 03-53 fl	Kråkemåla 2	Fluorite	1.76	7.83	0.1361	0.511689	–15.3
Kra 03-54 fl	Kråkemåla 1	Fluorite	6.23	19.22	0.1958	0.511862	–15.1
Kv 03-56 fl	SE of Kråkemåla	Fluorite	5.88	13.44	0.2643	0.512121	–13.8
Kv 03-57 fl	SE of Kråkemåla	Fluorite	9.79	20.56	0.2879	0.512263	–12.3
Kr 0417 wr	Kråkemåla 1	Götemar granite	2.40	19.35	0.0749	0.511341	–18.8
Kr 0418 wr	Kråkemåla 2	Götemar granite	8.92	64.53	0.0835	0.511441	–17.3
Tindered area							
Ti 03-38 fl	Tindered	Fluorite	7.72	19.05	0.2450	0.512009	–14.9
Ti 03-39 fl	Tindered	Fluorite	5.92	10.84	0.3302	0.512303	–13.8
Ti 03-40 fl	Tindered	Fluorite	7.40	14.76	0.3031	0.512216	–14.0
Ti 03-41 fl	Tindered	Fluorite	33.76	51.96	0.3927	0.512386	–15.5
Ti 03-42 fl	Tindered	Fluorite	3.94	10.04	0.2368	0.512021	–14.2
Ti 03-43 fl	Tindered	Fluorite	6.46	13.63	0.2865	0.512166	–14.1
Ti 03-44 fl	Tindered	Fluorite	66.14	117.41	0.3406	0.512266	–15.0
Ti 03-44B	Tindered	Calcite	24.74	117.57	0.1272	0.511699	–14.6
Ti 03-45 fl	Tindered	Fluorite	5.92	12.69	0.2819	0.512124	–14.7
Ti 03-46 fl	Tindered	Fluorite	8.41	16.97	0.2997	0.512216	–13.8
Ti 03-47 fl	Tindered	Fluorite	6.97	18.18	0.2316	0.512069	–13.0
Ti 0419 wr	Tindered	Porphyritic granite	10.09	46.84	0.1302	0.511917	–10.6
Ti 0420 wr	Tindered	Biotite granite	12.05	66.70	0.1092	0.511640	–14.8
Lovisa area							
Me 03-03 fl	Metsola	Fluorite	8.51	16.67	0.3087	0.512212	–14.4
Me 03-06 fl	Metsola	Fluorite	7.83	20.05	0.2362	0.512041	–13.8
Me 03-07 fl	Metsola	Fluorite	7.28	13.39	0.3286	0.512276	–14.2
Hv 03-08 fl	Hästholmsvägen	Fluorite	6.37	11.35	0.3390	0.512307	–14.2
Hv 03-09 fl	Hästholmsvägen	Fluorite	5.59	9.78	0.3458	0.512342	–13.8
Hv 03-10 fl	Hästholmsvägen	Fluorite	4.82	9.99	0.2919	0.512181	–14.1
Me 0401 wr	Metsola	Pyterlite	17.38	99.42	0.1057	0.511599	–15.4
Me 0403 wr	Metsola	Dark wiborgite	14.93	80.80	0.1117	0.511680	–14.2
Hv 0405 wr	Hästholmsvägen	Wiborgite	11.11	60.76	0.1106	0.511666	–14.4
Hv 0406 wr	Hästholmsvägen	Porphyry aplite	23.09	146.00	0.0956	0.511512	–16.6
Te 0407 wr	Tessjö/Tessjoki	Porphyry aplite	18.99	112.13	0.1024	0.511581	–15.6
Me 0408 wr	Metsola	Dark wiborgite	15.24	83.60	0.1102	0.511657	–14.6
Laisvall area							
Ak 2:1 fl	Ackerselet	Fluorite	5.18	17.44	0.1795	0.511900	–13.5
Ak 4:1 fl	Ackerselet	Fluorite	5.17	17.89	0.1748	0.511917	–12.9
Ak 5:1 fl	Ackerselet	Fluorite	1.78	8.35	0.1292	0.511786	–13.1
Ak 5:2 fl	Ackerselet	Fluorite	2.96	13.68	0.1307	0.511775	–13.4
Ak 6:1 fl	Ackerselet	Fluorite	3.96	12.92	0.1855	0.511941	–13.1
Ak 0415 wr	Ackerselet	Sorsele granite	18.68	86.86	0.1300	0.511707	–14.6
Ak 0421 wr	Ackerselet	Sorsele granite	9.91	51.42	0.1165	0.511701	–14.0

Error in 147Sm/144Nd is 0.4% (Ti03-44B 1%), and in 143Nd/144Nd 0.00001 (absolute 2 σ error).

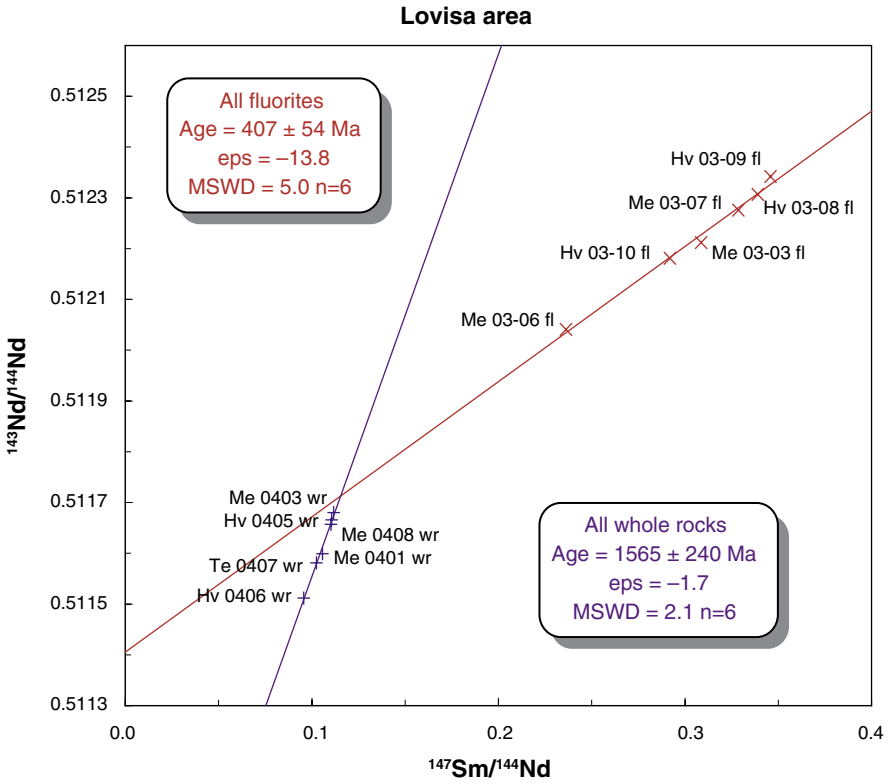

Figure 7-3. *Sm-Nd plot for fluorites and rocks, Lovisa area.*

Tindered area

For the Tindered fluorite population, a reference line with a slope corresponding to an age of 361 ± 77 Ma (MSWD = 40) can be constructed. If the data point generated by the calcite sample is included, a line corresponding to an age of 402 ± 57 Ma (MSWD = 47) is obtained (Figure 7-4). This age estimate can neither be improved by combining only the fluorite samples with the same host rock, nor by combining the fluorite samples with the data point generated by their respective host rock. A reference line for the coprecipitated fluorite-calcite pair corresponds to an age of 406 ± 10 Ma.

Götemar area

All five fluorite data points from the Götemar area generate a reference line with an age of 568 ± 180 (MSWD = 72). With the calcite sample included (Figure 7-5), the obtained age estimate is 538 ± 110 Ma (MSWD = 65). If the two fluorites hosted by TIB granitoids outside the Götemar granite are omitted, a line through the remaining three fluorite data points yields 414 ± 380 Ma (MSWD = 5.2) and if the calcite sample is included, 441 ± 87 Ma (MSWD = 6.1). A line connecting the fluorite-calcite pair yields an age estimate of 436 ± 18 Ma. No meaningful combinations with the two Götemar granite data points can be made.

Laisvall area

For the five Laisvall fluorites, a reference line corresponding to an age of 423 ± 130 Ma (MSWD = 8.0) is obtained (Figure 7-6). As for the Götemar data no meaningful combinations with the data points generated by the two Sorsele granite samples can be made.

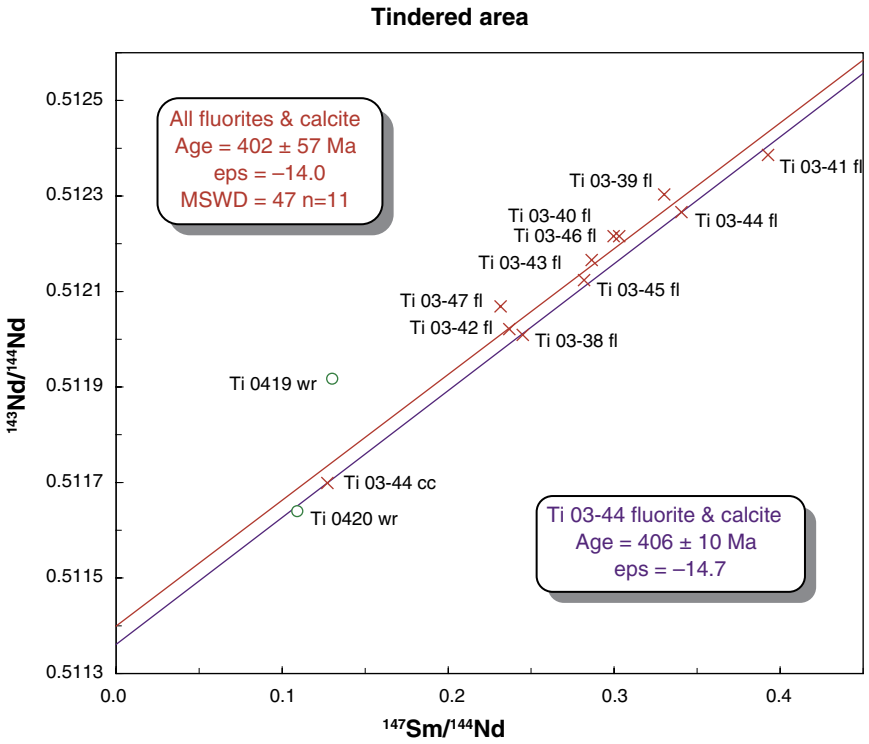

Figure 7-4. *Sm-Nd plot for fluorites, calcite and rocks, Tindered area.*

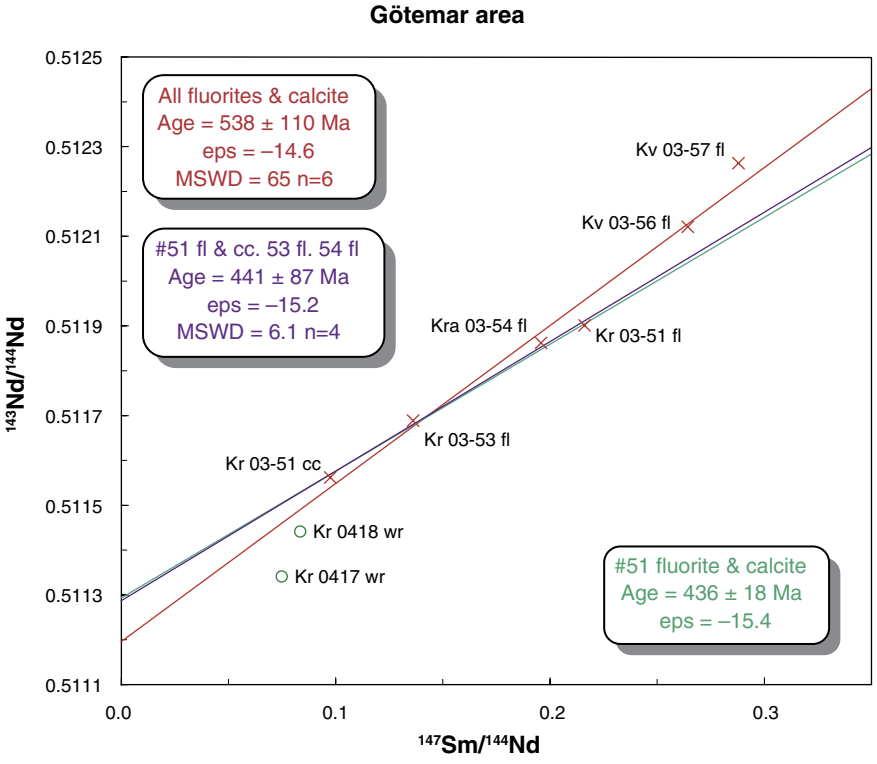

Figure 7-5. *Sm-Nd plot for fluorites, calcite and rocks, Götemar area.*

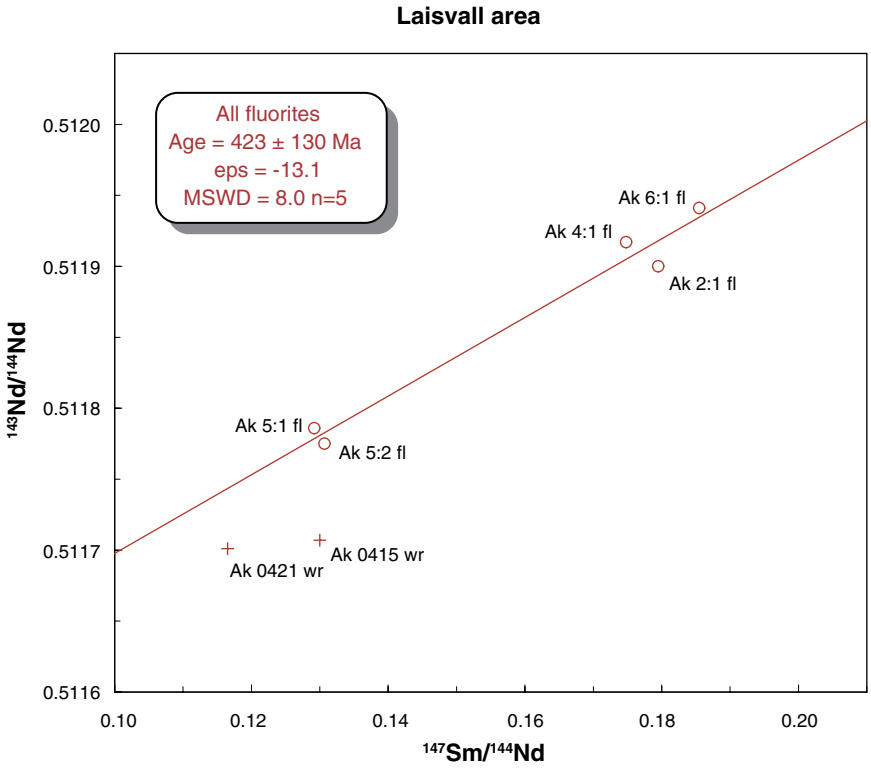

Figure 7-6. *Sm-Nd plot for fluorites and rocks, Ackerselet, Laisvall area.*

Total fluorite (and calcite) population

The total population of 28 mineral data, including vein fluorite as well as calcite and sandstone-cementing fluorite (Figure 7-7) yields a reference line corresponding to an age of 420 ± 35 Ma (MSWD = 78).

The various age estimates are summarized below:

Target area and sample association	Age (Ma)	MSWD
Götemar (three fluorites)	414 ± 380	5.2
Götemar (three fluorites and one calcite)	441 ± 87	6.1
Götemar (two fluorites from same quarry)	405 ± 27	–
Götemar (calcite-fluorite pair)	436 ± 18	–
Tindered (all 10 fluorites)	361 ± 77	40
Tindered (all 10 fluorites and one calcite)	402 ± 57	47
Tindered (calcite-fluorite pair)	406 ± 10	–
Lovisa (all 6 fluorites)	407 ± 54	5.0
Laisvall (all 5 fluorites)	423 ± 130	8.0
All targets (all 26 fluorites and two calcites)	420 ± 35	78

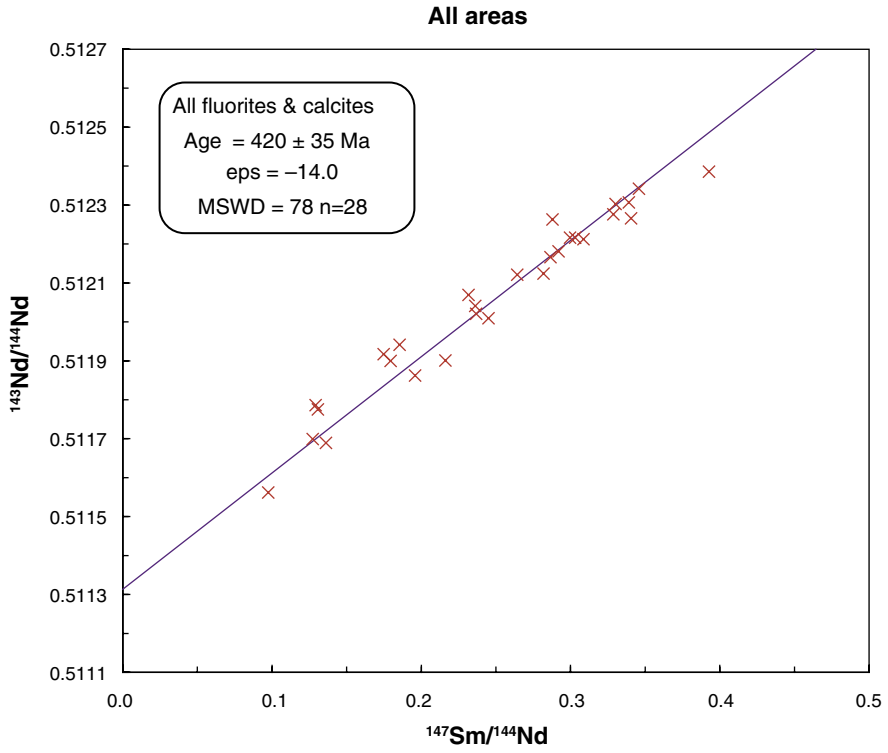

Figure 7-7. *Sm-Nd plot for fluorites and calcite, all areas.*

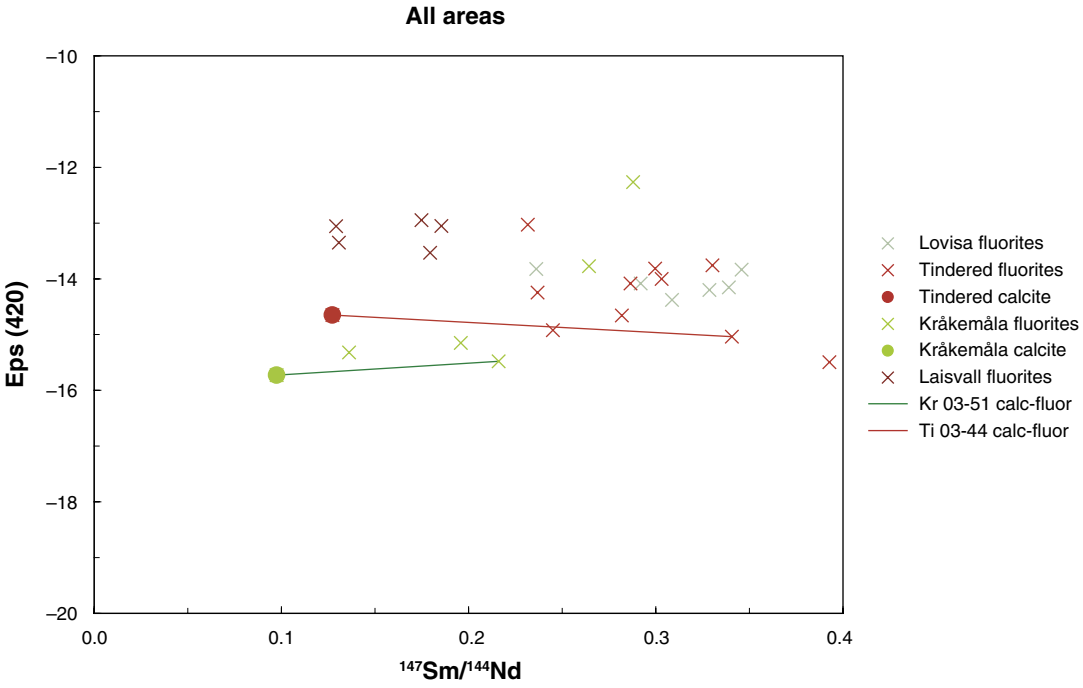

Figure 7-8. *$\varepsilon_{Nd(420\ Ma)}$ vs. $^{147}Sm/^{144}Nd$ plot for fluorites and calcites, all areas.*

8 Discussion

a. Geochemistry of potential source rocks

As was concluded by /Alm and Sundblad 2002/, the critical factor that governs the various proportions of fluorite, calcite and galena as well as the lead isotopic composition in each particular vein system is the geochemical character of the source rock.

One important element in this respect is F. In case there is insufficient F in the source rock, calcite is likely to be precipitated from the hydrothermal fluid. In low-F rocks, F is commonly tied to the crystal lattice of minerals like apatite, amphibole and pyroxene. In high-F rocks, e.g. evolved granites, these minerals will become saturated with F and fluorite will form in the rock. Based on available data for the F contents (/Alm and Sundblad 2002/ and this report), the Götemar granite has ≈ 0.4% F, the Tindered biotite granite ≈ 0.25% F, and, in the Lovisa area, the pyterlite ≈ 0.5% F and the porphyritic aplite ≈ 0.4% F. In most of these, magmatic fluorite is observed /Alm and Sundblad 2002/. The high F contents, and in particular the presence of magmatic fluorite, are probably the main reasons for the abundant occurrence of fluorite-dominated hydrothermal vein mineralization in the investigated areas, since a low-temperature fluid will release F easier from a fluorite-bearing rock than from a rock with all F tied to silicates or apatite. Each of these host rocks must therefore be considered as a realistic source for F in the low-temperature fluid that formed the veins, thus implying a very local derivation. Other host rocks, as the porphyritic granite in the Tindered area and wiborgites in the Lovisa area, have slightly lower F contents (0.12–0.25% F), and are thus less evident, but still possible, sources for the hydrothermal fluorites. The Sorsele granite constituting the basement for the Ackerselet Formation has such low F-content (≈ 0.05%), that it is an unlikely source for the fluorite in the above-lying sandstones. This provides support to models advocating long-transported fluids in the Laisvall system /Grip 1954, Rickard et al. 1979, Kendrick et al. 2005/.

The origin of Ca, as well as Sm and Nd, in the hydrothermal minerals is even more critical in the present context, because if the fluids contain elements from several sources, a complexity in the Sm-Nd isotope systematics of the hydrothermal mineral precipitate will arise. As noted above, two possible source rocks have been identified in the Tindered area and several possible source rocks in the Lovisa area, based on field criteria, available whole rock data on the F contents, and petrographic information. Each rock unit has its specific geochemical composition (see Appendix and /Gehör et al. 1997/) and variations in the initial $^{143}Nd/^{144}Nd$ ratios can be expected, which would cause a complex Sm-Nd isotope composition in the hydrothermal system. The conditions are even more complex in the Götemar area. While most of the investigated minerals are hosted by the Götemar granite, two fluorite samples were collected in the border zone to the TIB. Since these two samples have Sm-Nd isotope compositions that fall off the trend for the other samples from the Götemar area, it is assumed that the Sm and Nd compositions in these two samples were heavily influenced by the TIB granitoids. It is thus well-motivated to exclude the data points for these two samples from the age calculations. Furthermore, it is evident from a closer look at available chemical data from the Götemar intrusion that discrete geochemical variations exist within this intrusion, even if it appears to be reasonably homogeneous based on field criteria. As can be seen in Table 8-1, one variety of the Götemar granite, represented by five samples, has SiO_2 contents between 75.5 and 77.3%, and rather modest contents of several elements, e.g. Fe_2O_3tot, CaO, MgO, TiO_2, Sr, Sm and Nd, while another variety, represented

Table 8-1. Compositional range for selected elements in two Götemar granite types and TIB*.

	SiO2	Fe2O3tot	MgO	CaO	TiO2	Sr	Sm	Nd
Götemar								
Type 1 (n=5)	75.5–77.3	0.70–1.25	0.06–0.12	0.44–0.75	0.05–0.11	28–73	2.5–5.0	20–28
Type 2 (n=4)	72.0–74.1	1.88–2.23	0.32–0.43	1.04–1.18	0.27–0.33	127–130	6.4–9.3	49–61
TIB (n=8)	69.0–71.1	2.61–3.58	0.75–1.23	1.93–2.59	0.36–0.51	530–798	4.9–7.4	32–50

Oxides are given as weight percent, trace elements as ppm.

*Data from this report and /Wikman and Kornfält 1995/.

by four samples, has SiO_2 contents between 72.0 and 74.1%, and significantly higher contents of the other mentioned elements, thus indicating the presence of two magmatic suites within the Götemar pluton. Even if it is beyond the scope of this investigation to speculate in the reason for this bimodality, it cannot be excluded that these geochemical variations are accompanied by variations in the initial $^{143}Nd/^{144}Nd$ ratios. Considerable care should thus be taken when evaluating the Sm-Nd isotope data even for individual target areas.

b. Fluid inclusion characteristics and geochemistry of fluorites

Fluid inclusion investigations of the fluorite-calcite-galena veins in the Baltic Sea region indicated depositional temperatures of 100–150°C /Alm and Sundblad 2002/, which is comparable to the estimates made for the fluorite-calcite-galena veins /Johansson 1980/ and the sandstone-hosted mineralization /Lindblom 1982/ along the Caledonian front.

From the fluid inclusion study by /Alm and Sundblad 2002/, indications of two fluids with different salinities were obtained in fluorites from the Tindered and Götemar areas. An influx of fluids with slightly different compositions may have entered the fracture systems at some discrete occasions during vein formation, although probably not widely separated in time. The obvious variation in initial $^{143}Nd/^{144}Nd$ ratios within the fluorite populations may arise from such inhomogeneities in fluid composition. However, the fluid inclusion data are obtained from a few grains of fluorite and calcite at each locality. The REE compositions obtained for bulk samples are in general very similar, implying a similar source. One exception is the Tindered sample # 44, with its deviating pattern (Figure 7-2b). This behaviour may be connected with the fact that this fluorite was intergrown with abundant calcite and therefore a result of fractionation between the two REE-bearing phases. Details about such fractionation are not discussed here.

When the REE profiles for fluorites are compared to those of the rocks in the Tindered and Lovisa areas respectively, a similar change of the pattern is revealed for both areas. The LREE are depleted in the fluorites compared to the rocks, whereas the MREE are significantly enriched and the HREE less enriched. /Schwinn and Markl 2005/ have shown that leaching of granites by a fluid, and subsequent precipitation of fluorite from this fluid produces a similar change in the REE pattern as that obtained in this study. It may therefore be inferred that the local granites in the Tindered and Lovisa areas constitute the source for trace elements to the hydrothermal fluids that deposited the fluorite. For the Götemar area the few available REE data are not enough conclusive in this respect. The fractionation trend, with (MREE)HREE enrichment relative to the LREE displayed in all investigated areas, may be due to variations in the complexing behaviour between LREE and HREE in the hydrothermal fluid, as suggested by e.g. /Möller and Morteani 1983/.

c. Age constraints of the fluorite-calcite-galena mineralization

The age of the fluorite-calcite-galena mineralization has been discussed for more than fifty years and a wide range of ages has been proposed /e.g. Grip 1954, Tegengren 1962, Bjørlykke and Thorpe 1982, Larson and Tullborg 1998/. Although a Phanerozoic age is evident from the geological relations between the mineralization and the Cambrian sandstone, there are few firm data available to provide a more detailed timing. The highly radiogenic lead isotopic compositions of galena in veins /Johansson 1983, Alm and Sundblad 2002/ and sandstones /Rickard et al. 1981/ yield negative model ages, typical for a Phanerozoic reactivation of Precambrian crustal sources, but of little use for more precise age determination.

A Late Palaeozoic formation of the hydrothermal system, as a result of increased thermal conditions created by the Devonian sediment accumulation, was proposed by /Larson and Tullborg 1998/. This model is, however, questioned by the similarity in depositional temperature, determined from fluid inclusions, for fluorite-calcite-galena veins close to the Caledonian front /Johansson 1980/, and in the Baltic Sea region /Alm and Sundblad 2002/. In case the increased heat flow and associated hydrothermal activity were generated by thick piles of post-Caledonian sediments, the various mineralizations should record differing fluid inclusion characteristics, particularly when considering the highly variable depth estimates obtained for different parts of the Devonian foreland basin /Middleton et al. 1996, Samuelsson and Middleton 1998, Larson et al. 1999/. Serious doubts about a burial-generated model /Larson and Tullborg 1998/ is also raised because it cannot explain the intense fracturing associated with the hydrothermal activity. A mineralization process independent of a thick overburden is therefore suggested.

Although no proper Sm-Nd isochrons were obtained for the investigated fluorites, individual fluorite (and calcite) populations, representing well-defined geological environments, display linear trends that can be evaluated with respect to ages (Figures 7-3–7-6). The most reliable of those are the two fluorite-calcite pairs analyzed for Götemar and Tindered, since the two minerals in each pair must have formed semicontemporaneously from the same hydrothermal fluid. The $\varepsilon_{Nd\ (420\ Ma)}$ vs. $^{147}Sm/^{144}Nd$ diagram (Figure 7-8) gives support for such an assumption because data for coprecipitated minerals should form horizontal lines in such a diagram. The ages calculated for these two mineral pairs are 436 ± 18 Ma for Götemar and 406 ± 10 Ma for Tindered. Age calculations based on other geologically motivated groupings of data (including samples from the same quarry in Götemar as well as the entire fluorite ± calcite populations in Tindered, Lovisa and Laisvall) give similar results, although with larger errors. An age calculation made on data for the two fluorites and one coexisting calcite from the same quarry gives 432 ± 310 Ma. This large error may be caused by the geochemical variations detected within the Götemar pluton (see above). Furthermore, if the total mineral data population from all four target areas (thus evidently involving numerous sources) are included in one calculation, an age of 420 ± 35 Ma is obtained. Even if the obtained ages are imprecise, they all provide independent indications towards ages in the range between 400 and 440 Ma, suggesting shield-scale hydrothermal and tectonic event(s) during the Silurian to Early Devonian. These data do not support the burial-generated model (Permian) for the vein mineralization as proposed by /Larson and Tullborg 1998/ nor the the syngenetic model (Cambrian) for the sandstone mineralization as proposed by /Bjørlykke and Thorpe 1982/, and some alternative processes and events must be found to explain the shield-scale tectonic and hydrothermal activity.

The Lochkovian/Pragian system of faults and fractures in Latvia and Estonia is a very strong and concrete piece of evidence for a dramatic and episodic impact on the Precambrian crust and overlying sedimentary sequence in the Early Devonian. The geometry of these faults and fractures coincide with the main trend for the fluorite-calcite-galena-bearing fractures in the Baltic Sea region, and are also sub-parallel to a suspect horst-graben system in the Lovisa area. Since the timing of the Latvian fault systems (410–415 Ma) is based on fossil evidence and well-established geochronological calibrations, it is constrained to within a few million years. This age is in excellent agreement with the (less well-constrained) Sm-Nd ages obtained for the mineralized fractures in the Baltic Sea region. Based on these temporal and structural similarities, it is suggested that the Lochkovian/Pragian fault systems in Latvia and Estonia were formed semicontemporaneously with the fracture-controlled fluorite-calcite-galena mineralizations in the Baltic Sea region. In consequence, the true age of this hydrothermal system should be close to 410–415 Ma.

The 423 ± 130 Ma age for the Laisvall fluorites is the first radiometric age estimate of the galena-fluorite-calcite paragenesis in this major ore system. It is consistent with the much more precise age determinations of lead mobilization (420 ± 3 Ma) in the interior of the Caledonides /Stuckless et al. 1982/ and K-feldspar overgrowths (430 ± 4 Ma and 424 ± 4 Ma) in Laisvall /Kendrick et al. 2005/. Thus, the imprecise Sm-Nd age estimate for the Ackerselet fluorites is nevertheless realistic and it is suggested that a true age for the hydrothermal event in Laisvall is close to 420–430 Ma. The combined evidence of the timing and the long-transported character of the hydrothermal system in Laisvall lend support to the genetic models for Laisvall suggested by /Grip 1954, Rickard et al. 1979, Kendrick et al. 2005/ but are not compatible with the model proposed by /Bjørlykke and Thorpe 1982/ for the Osen sandstone-hosted deposit. It is worth noting that if all pieces of evidence are combined, they indicate that the hydrothermal fluids forming the Laisvall sandstone-hosted deposit are distal (e.g. /Kendrick et al. 2005/ and this report) while the hydrothermal fluids forming the veins in the Baltic Sea region are proximal (/Alm and Sundblad 2002/ and this report). Based on the arguments by /Bjørlykke and Thorpe 1982/ the Osen deposit should have formed by local fluids. Without further investigations on the calcite-fluorite veins along the Caledonian front and the scattered occurrences of sandstone-hosted mineralization in the Baltic Sea region, it remains unclear whether this difference is type-related or region-related.

d. Geodynamic implications

As shown above, the combined information on the geological setting, fluid inclusion systematics and Sm-Nd data suggest a Late Silurian/Early Devonian age for the fluorite-calcite-galena mineralizations. If the precise ages provided by /Stuckless et al. 1982/ and /Kendrick et al. 2005/ are considered relevant for the Laisvall mineralization (i.e. 420–430 Ma) and the Lochkovian/Pragian (i.e. 410–415 Ma) age is considered relevant for the veins in the Baltic Sea region, it is implied that the hydrothermal activity along the Caledonian front preceded the hydrothermal system in the Baltic Sea region with some 5 to 10 million years. This time discrepancy is consistent with a south-eastwards migrating foreland basin as proposed by /Basset 1985/ in the Late Silurian/Early Devonian. The most plausible geodynamic scenario for the shield-scale low-temperature hydrothermal mineralization is therefore that the Caledonian continent-continent collision was accompanied by an extensional tectonic regime in the foreland /cf. Jordan 1981, Tankard 1986/ resulting in upbulging of the lithosphere, fracturing of the upper parts of the Precambrian crust as well as uplift and erosion of the Cambro-Silurian and Lochkovian platform sediments.

9 Conclusions

The Sm-Nd isotope results on low-temperature hydrothermal fluorite (and calcite) in veins in the Baltic Sea region and fluorite in sandstones along the Caledonian front indicate local variations in the initial $^{143}Nd/^{144}Nd$ ratios. Such variations limit the possibility to use the Sm-Nd isotope technique on the fluorite (and calcite) for age determinations and no proper Sm-Nd isochrons were obtained. Sm-Nd data were also generated on a set of potential source rocks to the hydrothermal systems in order to improve the age calculations but this attempt did not prove to be successful.

Nevertheless, individual fluorite (and calcite) populations, representing well-defined geological environments, display linear trends that can be evaluated with respect to ages. The most reliable and precise age estimates were obtained by analyzing coprecipitated mineral pairs (fluorite and calcite). Sm-Nd isotope age calculations, using other geologically relevant sample populations, resulted in similar ages, although with less precision, indicating shield-scale hydrothermal activity in the Silurian to Early Devonian. This activity took place in conjunction with major fault tectonics reaching many hundreds of metres below the subcambrian peneplain.

Comparison with well-dated lead mobilization in the interior of the Caledonides and K-feldspar associated with mineralization in the Caledonian front suggest that the hydrothermal activity in the Caledonides took place at 420–430 Ma (Wenlock/Ludlow).

Comparison with well-dated regional fracture systems in Latvia suggest that the low-temperature hydrothermal veins in the Baltic Sea region were formed in conjunction with faulting, uplift and the transition from marine to fluvial sedimentary conditions during the Lochkovian to Pragian, i.e. at c 410–415 Ma, some 5–10 m.y. later than the hydrothermal event in the Caledonides.

The time lag between the hydrothermal activity in these two environments is in accordance with sedimentological evidence for an advancing Caledonian thrust front and a south-eastwards migrating foreland basin during the Late Silurian to the Early Devonian.

The hydrothermal processes operated over the entire Fennoscandia and produced the largest (and most economic) concentrations of galena in Europe (Laisvall and Vassbo along the Caledonian front). Similar and semicontemporaneous ore forming processes were also active elsewhere in Fennoscandia and a possibility to discover similar concentrations in the Cambrian successions in the Baltic Sea region cannot be excluded. A key problem is that far-transported hydrothermal solutions may be necessary for creating large enough metal concentrations, an incident that may be unique for the hydrothermal deposits along the Caledonian front.

10 Acknowledgements

This study was financed by the Swedish Nuclear Fuel and Waste Management Co (SKB). High quality assistance in the isotope laboratory was received from Tuula Hokkanen (chemistry) and Arto Pulkkinen (mass-spectrometry). Mats Willdén, Boliden, kindly provided important unpublished information on the Ackerselet deposit. Jerry Hedström and his colleagues at the Mineral Office of the Geological Survey of Sweden, Malå, provided excellent service in giving access to drillcores and miscellaneous information. D. Gee, Uppsala, and D. Sollien, Stavanger, are thanked for valuable comments on an early version of the report.

11 References

Alm E, Sundblad K, 2002. Fluorite-calcite-bearing fractures in the counties of Kalmar and Blekinge, Sweden. SKB R-02-42, 116 pp, Svensk Kärnbränslehantering AB.

Alm E, Huhma H, Sundblad K, 2004. Preliminary Palaeozoic Sm-Nd ages of fluorite-calcite-galena veins in the southeastern part of the Fennoscandian Shield. SKB R-04-27. Svensk Kärnbränslehantering AB.

Bassett M G, Cherns L, Karis L, 1982. The Röde formation; Early Old Red Sandstone facies in the Silurian of Jämtland, Sweden. Sveriges Geologiska Undersökning C 793, 24 pp.

Bassett M G, 1985. Silurian stratigraphy and facies development in Scandinavia. In: D.G. Gee & B.A. Sturt (eds.): The Caledonide Orogen – Scandinavia and related areas. John Wiley and Sons Ltd, 283–292.

Bergman L, 1982. Clastic dykes in the Åland islands, SW Finland and their origin. Geological Survey of Finland, Bulletin 317, 7–33.

Bergström J, Gee D G, 1985. The Cambrian in Scandinavia. In: D.G. Gee & B.A. Sturt (eds.): The Caledonide Orogen – Scandinavia and related areas. John Wiley and Sons Ltd, 247–271.

Beunk F F, Page L M, 2001. Structural evolution of the accretional continental margin of the Paleoproterozoic Svecofennian orogen in southern Sweden. Tectonophysics 339, 67–92.

Bjørlykke A, Sangster D F, 1981. An overview of sandstone lead deposits and their relation to red-bed copper and carbonate-hosted lead-zinc deposits. Economic Geology 75th Anniversary volume, 179–213.

Bjørlykke A, Thorpe R 1, 1982. The source of lead in the Osen sandstone lead deposit on the Baltic Shield, Norway. Economic Geology 77, 430–440.

Bjørlykke A, 1983. Sulphur isotopic composition of the sandstone-lead deposits in southern Norway. Norges Geologiske Undersøkelse, Bulletin 380, 143–158.

Bjørlykke A, Ihlen P M, Olerud S, 1990. Metallogeny and lead isotope data from the Oslo Paleorift. Tectonophysics 178, 109–126.

Boynton W V, 1984. Cosmochemistry of the rare earth elements: meteorite studies. In: P. Henderson (ed.): Rare earth element geochemistry, Elsevier, pp 63–114.

Braathen A, Osmundsen P T, Nordgulen Ø, Roberts D, Meyer G B, 2002. Orogen-parallel extension of the Caledonides in northern Central Norway: an overview. Norsk Geologisk Tidsskrift 67, 225–241.

Brangulis A J, Kurss V, Misans J, Stinkulis G, 1998. Latvijas geologija. State Geological Survey of Latvia, 70 pp.

Brangulis A J, Kanevs S, 2002. Latvijas tektonika. State Geological Survey of Latvia, 50 pp.

Bruton D L, Lindström M, Owen A W, 1985. The Ordovician of Scandinavia. In: D.G. Gee & B.A. Sturt (eds.): The Caledonide Orogen – Scandinavia and related areas. John Wiley and Sons Ltd, 273–282.

Carlsson L, 1970. Blymalmen i Laisvall. Sambandet mellan mineraliseringar, tektonik, sedimentologi och paleogeografi. Unpubl. Licenciate Thesis, Stockholm University, 31 pp.

Claesson S, Roddick J C, 1983. $^{40}Ar/^{39}Ar$ data on the age and metamorphism of the Ottfjället dolerites, Särv Nappe, Swedish Caledonides. Lithos 16, 61–73.

Claesson S, Stephens M B, Klingspor I, 1988. U-Pb zircon dating of felsic intrusions, Middle Köli Nappes, central Swedish Caledonides. Norsk Geologisk Tidsskrift 68, 89–97.

Chesley J T, Halliday A N, Scrivener R C, 1991. Samarium-neodymium direct dating of fluorite mineralization. Science 252, 949–951.

Chesley J T, Halliday A N, Kyser T K, Spry P G, 1994. Direct dating of Mississippi Valley-Type mineralization: use of Sm-Nd in fluorite. Economic Geology 89, 1192–1199.

Christoffersson H C, Wallin B, Selkman S, Rickard D T, 1979. Mineralization controls in the sandstone lead-zinc deposits at Vassbo, Sweden. Economic Geology 74, 1239–1249.

Cox K G, Bell J D, Pankhurst R J, 1979. The interpretation of igneous rocks. Allen and Unwin, London. 450 pp.

Debon F, Le Fort P, 1982. A chemical-mineralogical classification of common plutonic rocks and associations. Transactions of the Royal Society of Edinburgh: Earth Sciences 73, 135–149.

Dunning G R, Pedersen R B, 1988. U/Pb ages of ophiolites and arc-related plutons of the Norwegian Caledonides: implications for the development of the Iapetus. Contributions to Mineralogy and Petrology 98, 13–23.

Fossen H, Rykkelid E, 1992. Postcollisional extension of the Caledonide orogen in Scandinavia: Structural expressions and tectonic significance. Geology 20, 737–740.

Gaál G, Gorbatschev R, 1987. An outline of the Precambrian evolution of the Baltic Shield. Precambrian Research 35, 15–52.

Galindo C, Tornos F, Darbyshire D P F, Casquet C, 1994. The age and origin of the barite-fluorite (Pb-Zn) veins of the Sierra del Guadarrama (Spanish Central System, Spain): a radiogenic (Nd, Sr) and stable isotope study. Chemical Geology (Isotope Geoscience Section) 112, 351–364.

Gehör S, Kärki A, Taikina-aho O, 1997. Loviisan Hästholmenin kairausnäytteiden petrologia ja matalan lämpötilan rakomineraraalit. Työraportti-97-36, Posiva, Helsinki, 207 pp.

Gradstein F M, Ogg J G, Smith A G (coordinators), Agterberg F P, Bleeker W, Cooper R A, Davydov V, Gibbard P, Hinnov L A, House M R, Lourens L, Luterbacher H-P, McArthur J, Melchin M J, Robb L J, Shergold J, Villeneuve M, Wardlaw B R, Ali J, Brinkhuis H, Hilgen F J, Hooker J, Howarth R J, Knoll A H, Laskar J, Monechi S, Powell J, Plumb K A, Raffi I, Röhl U, Sadler P, Sanfilippo A, Schmitz B, Shackleton N J, Shields G A, Strauss H, Van Dam J, Veizer J, van Kolfschoten Th, Wilson D, 2004. A Geologic Time Scale 2004. Cambridge University Press, 610 pages.

Grip E, 1954. Blymalmen vid Laisvall, dess geologi och en jämförelse med några utländska förekomster. Geologiska Föreningens i Stockholm Förhandlingar 76, 357–380.

Grip E, 1967. On the genesis of lead ores of the eastern border of the Caledonides in Scandinavia. Economic Geology Monography 3, 208–217.

Grip E, 1973. Sulfidmalm i fjällkedjan och i det baltiska kambriska flackhavsområdet. In: E. Grip & R. Frietsch: Malm i Sverige 2. Almqvist & Wiksell, Stockholm, 10–66.

Hanski E, Huhma H, Rastas P, Kamenetsky V S, 2001. The Palaeoproterozoic komatiite-picrite association of Finnish Lapland. Journal of Petrology 42 (5), 855–876.

Hossack J R, 1984. The geometry of listric growth faults in the Devonian basins of Sunnfjord, W Norway. Geological Society of London Journal 141, 629–637.

Huhma H, Mutanen T, Whitehouse M, 2004. Oldest rocks of the Fennoscandian Shield; The 3.5 Ga Siurua trondhjemite gneiss in the Archaean Pudasjärvi Granulite Belt, Finland. GFF 126, p. 17.

Johansson Å, 1980. Fluid inclusion thermometry on calcite, sphalerite and fluorite from the Åkerlandet vein, Västerbotten County. In: D. Rickard (ed.) Annual Report of the Ore Research Group, Stockholm University, 188–200.

Johansson Å, Rickard D, 1982. The Variscian lead-zinc-fluorite veins of southern Sweden. Bulletin du BRGM (2) II 2, 133–142.

Johansson Å, 1983. Lead isotopic composition of Caledonian sulfide-bearing veins in Sweden. Economic Geology 78, 1674–1688.

Jordan T E, 1981. Thrust loads and foreland basin evolution, Cretaceous, western United States. Bull. American Association of Petroleum Geology 65, 2506–2520.

Kendrick M A, Burgess R, Harrison D, Bjørlykke A, 2005. Noble gas and halogen evidence for the origin of Scandinavian sandstone-hosted Pb-Zn deposits. Geochimica et Cosmochimica Acta 69, 109–129.

Kleesment A, Mark-Kurik E, 1997. Devonian sedimentary cover: Lower and Middle Devonian. In: A. Raukas & A. Teedumäe (eds.) Geology and Mineral Resources of Estonia. Estonian Academy Publishers, Tallinn, 107–121.

Kresten P, Chyssler J, 1976. The Götemar massif in south-eastern Sweden: A reconnaissance survey. Geologiska Föreningens i Stockholm Förhandlingar 98, 155–161.

Kumpulainen R, Nystuen J P, 1985. Late Proterozoic basin evolution and sedimentation in the westernmost part of Baltoscandia. In: D.G. Gee & B.A. Sturt (eds.): The Caledonide Orogen – Scandinavia and related areas. John Wiley and Sons Ltd, 213–232.

Kurss V M, 1992. Devonian terrigeneous deposition in the main devonian field. Zinatne, Riga, 208 pp. [In Russian].

Laitakari I, Simonen A, 1962. Geological map of Finland in scale 1:100,000, Pre-Quaternary rocks, sheet 3022 Lapinjärvi. Geological Survey of Finland.

Laitala M, 1964. Geological map of Finland in scale 1:100,000, Pre-Quaternary rocks, sheets 3021 Porvoo. Geological Survey of Finland.

Larson S Å, Tullborg E-L, 1998. Why Baltic Shield zircons yield late Paleozoic, lower intercept ages on U-Pb concordia. Geology 26, 919–922.

Larson S Å, Tullborg E-L, Cederbom C, Stiberg J-P, 1999. Sveconorwegian and Caledonian foreland basins in the Baltic Shield revealed by fission-track thermochronology. Terra Nova 11, 210–215.

Lidmar-Bergström K, 1996. Long term morphotectonic evolution in Sweden. Geomorphology 16, 33–59.

Lilljequist R, 1973. Caledonian geology of the Laisvall area, southern Norrbotten, Swedish Lapland. Sveriges Geologiska Undersökning C 691, 43 pp.

Lindblom S, 1982. Fluid inclusion studies of the Laisvall sandstone lead-zinc deposit, Sweden. Meddelanden från Stockholms Universitets Geologiska Institution 252, 171 pp.

Ludwig K R, 2001. Isoplot/Ex rev. 2.49. A Geochronological Toolkit for Microsoft Excel. Berkeley Geochronology Center, Special Publication No. 1a. 55 pp.

Lundegårdh P H, Wikström A, Bruun Å, 1985. Provisoriska översiktliga berggrunds-kartan Oskarshamn i skala 1:250000. Sveriges Geologiska Undersökning Ba 34.

Mattsson Å, 1962. Morphologische Studien in Südschweden und auf Bornholm über die nichtglaziale Formenwelt der Felsenskulptur. Lund studies in Geography, ser. A. Physical Geography 20, 357 pp.

Mens K, Pirrus E, 1997. Vendian-Tremadoc clastogenic sedimentation basins. In: A. Raukas & A. Teedumäe (eds.) Geology and Mineral Resources of Estonia. Estonian Academy Publishers, 184–191.

Menuge J F, Feely M, O'Reilly C, 1997. Origin and granite alteration effects of hydro-thermal fluid: isotopic evidence from fluorite veins, Co. Galway, Ireland. Mineralium Deposita 32, 34–43.

Middleton M F, Tullborg E-L, Larson S Å, Björklund L, 1996. Modelling of a Caledonian foreland basin in Sweden: petrophysical constraints. Marine and Petroleum Geology 13, 407–413.

Murnieks A, 1999. Geological map of Latvia in scale 1:200,000, pre-Quaternary deposits; sheet 42 Jurmala. Ministry of Environmental Protection and Regional Development, State Geological Survey of Latvia.

Möller P, Morteani G, 1983. On the geochemical fractionation of rare earth elements during the formation of Ca-minerals and its application to the problems of the genesis of ore deposits. In: Augustithis S.S. (ed.): The significance of trace elements in solving petroge-netic problems and controversies. Theophrastus Publications, Athens, pp 747–791.

Nestor H, Einasto R, 1997. Ordovician and Silurian carbonate sedimentation basin. In: A. Raukas & A. Teedumäe (eds.) Geology and Mineral Resources of Estonia. Estonian Academy Publishers, 192–204.

Neumann E-R, Olsen K H, Baldridge W S, Sundvoll B, 1992. The Oslo Rift: a review. Tectonophysics 208, 1–18.

Nikishin A M, Ziegler P A, Stephenson R A, Cloetingh S A P L, Furne A V, Fokin P A, Ershov A V, Bolotov S N, Korotaev M V, Alekseev A S, Gorbachev V I, Shipilov E V, Lankreijer A, Bembinova E Yu, Shalimov I V, 1996. Late Precambrian to Triassic history of the East European Craton: dynamics of sedimentary basin evolution. Tectonophysics 268, 23–63.

Norton M G, McClay K R, Way N A, 1987. Tectonic evolution of Devonian basins in northern Scotland and southern Norway. Norsk Geologisk Tidsskrift 67, 323–338.

Puura V, Vaher R, 1997. Cover structure. In: A. Raukas & A. Teedumäe (eds.) Geology and Mineral Resources of Estonia. Estonian Academy Publishers, 167–177.

Rickard D T, Willdén M Y, Marinder N-E, Donnely T H, 1979. Studies on the genesis of the Laisvall lead-zinc deposit, Sweden. Economic Geology 74, 1255–1285.

Rickard D, Coleman M, Swainbank I, 1981. Lead and sulfur isotopic compositions of galena from the Laisvall sandstone lead-zinc deposit, Sweden. Economic Geology 76, 2042–2046.

Samuelsson J, Middleton M F, 1998. The Caledonian foreland basin in Scandinavia: constrained by the thermal maturation of the Alum Shale. GFF 120, 307–314.

Schwinn G, Markl G, 2005. REE systematics in hydrothermal fluorite. Chemical Geology 216, 225–248.

Simonen A, 1965. Geological map of Finland in scale 1:100,000, Pre-Quaternary rocks, sheet 3024 Karhula. Geological Survey of Finland.

Simonen A, Laitala M, 1970. Geological map of Finland in scale 1:100,000, Pre-Quaternary rocks, sheets 3023 + 3014 Kotka. Geological Survey of Finland.

Skiöld T, 1988. Implications of new U-Pb zircon chronology to early Proterozoic crustal accretion in northern Sweden. Precambrian Research 38, 147–164.

Smellie J A T, Stuckless J S, 1985. Element mobility studies of two drill-cores from the Götemar granite (Kråkemåla test site), southeast Sweden. Chemical Geology 51, 55–78.

Steel R, Siedlecka A, Roberts D, 1985. The Old Red Sandstone basins of Norway and their deformation: a review. In D.G. Gee & B.A. Sturt (eds.): The Caledonide Orogen – Scandinavia and related areas. John Wiley and Sons, 293–315.

Stephens M B, Gee D G, 1989. Terranes and polyphase accretionary history in the Scandinavian Caledonides. In: R.D. Dallmeyer (ed.) Terranes in the Circum-Atlantic Paleozoic orogens. Geological Society of America Special Paper 230, 17–30.

Stuckless J S, Troeng B, Hedge C E, Nkomo I T, Simmons K R, 1982. Age of uranium mineralization at Lilljuthatten in Sweden and constraints on ore genesis. Sveriges Geologiska Undersökning C 798, 49 pp.

Sundblad K, Alm E, 2000. Flusspatförande spricksystem i den prekambriska berggrunden i Östersjöregionen. Unpublished report to SKB, 35 pp. Svensk Kärnbränslehantering AB.

Sundblad K, Alm E, Huhma H, Vaasjoki M, Sollien D B, 2004. Early Devonian tectonic and hydrothermal activity in the Fennoscandian Shield: evidence from calcite-fluorite-galena mineralization. In: S. Mertanen (ed.), Extended Abstract volume, Supercontinents, remagnetizations and geomagnetic modelling, 5th Nordic Paleomagnetic Workshop and Symposium, Helsinki, 2004. Geologian Tutkimuskeskus, Espoo. Report Q29,1/2004/1, 67–71.

Svenningsen O M, 2001. Onset of sea floor spreading in the Iapetus Ocean at 608 Ma: precise age of the Sarek Dyke Swarm, northern Swedish Caledonides. Precambrian Research 110, 241–254.

Tankard A J, 1986. On the depositional response to thrusting and lithosphere flexure: examples from the Appalachian and Rocky Mountain basins. In: P.A. Allen & P. Homewood (eds.) Foreland Basins. Spec. Publ. Int. Assoc. Sedimentol. 8, 369–394.

Tegengren F R, 1962. Vassbo blymalmsfyndighet i Idre och dess geologiska inramning. Sveriges Geologiska Undersökning C 586, 61 pp.

Torsvik T H, Smethurst M A, Meert J G, van der Voo R, McKerrow W S, Brasier M D, Sturt B A, Walderhaug H J, 1996. Continental break-up and collision in the Neoproterozoic and Palaeozoic; a tale of Baltica and Laurentia. Earth-Sciences Reviews 40, 229–258.

Tullborg E-L, Larson S Å, Björklund L, Samuelsson L, Stigh J, 1995. Thermal evidence of Caledonide foreland, molasse sedimentation in Fennoscandia. SKB TR 95-18, 38 pp, Svensk Kärnbränslehantering AB.

Turner P, Whitaker J H McD, 1976. Petrology and provenance of the late Silurian fluvial sandstones from the Ringerike Group of Norway. Sedimentary Geology 16, 45–68.

Vaasjoki M, Rämö O T, Sakko M, 1991. New U-Pb ages from the Wiborg rapakivi area: constraints on the temporal evolution of the rapakivi granite – anorthosite – diabase dyke association of southeastern Finland. Precambrian Research 51, 227–243.

Vidal G, Moczydlowska M, 1995. The Neoproterozoic of Baltica – stratigraphy, palaeobiology and general geological evolution. Precambrian Research 73, 197–216.

Wikman H, Kornfält K-A, 1995. Updating of a lithological model of the bedrock of the Äspö area. SKB Progress Report 25-95-04, 42 pp, Svensk Kärnbränslehantering AB.

Willdén M Y, 1980. Paleoenvironment of the autochthonous sedimentary rock sequence at Laisvall, Swedish Caledonides. Stockholm Contributions in Geology 33, 100 pp.

Åberg G, 1988. Middle Proterozoic anorogenic magmatism in Sweden and worldwide. Lithos 21, 279–289.

Åberg G, Löfvendahl R, Levi B, 1984. The Götemar granite – isotopic and geochemical evidence for a complex history of an anorogenic granite. Geologiska Föreningens i Stockholm Förhandlingar 106, 327–333.

Åhäll K-I, 2001. Åldersbestämning av svårdaterade bergarter i sydöstra Sverige. SKB R-01-60, 28 pp, Svensk Kärnbränslehantering AB.

Appendix

Chemical composition of rocks

	Götemar		Tindered		Lovisa								Laisvall	
	Kr 0417	Kr 0418	Ti 0419	Ti 0420	Me 0401	Me 0402	Me 0403	Me 0408	Me 0404	Me 0409	Hv 0405	Hv 0406	Te 0407*	Ak 0415	Ak 0421
SiO2	76.76	72.39	71.05	76.43	75.69	74.92	65.41	67.07	70.20	69.59	70.75	73.33	74.46	67.39	67.73
Al2O3	12.66	14.15	13.88	11.72	12.22	12.42	15.60	15.05	13.95	13.94	14.30	12.69	12.54	14.48	14.31
Fe2O3 tot	0.97	1.88	3.88	2.35	2.49	2.74	6.06	5.36	4.36	4.65	3.45	3.13	2.80	4.91	4.70
MgO	0.08	0.32	0.49	0.18	0.07	0.08	0.32	0.40	0.28	0.40	0.28	0.10	0.13	1.06	0.72
CaO	0.66	1.04	1.54	0.81	0.86	1.08	3.62	2.71	1.88	1.75	1.25	0.69	0.74	1.13	1.39
Na2O	3.69	3.76	3.08	2.83	2.49	2.53	2.95	2.69	2.87	2.94	2.88	2.60	2.65	3.31	3.68
K2O	4.67	5.49	5.11	4.82	5.30	5.29	4.54	4.97	5.14	5.38	5.93	5.82	5.58	5.03	4.80
TiO2	0.08	0.27	0.44	0.19	0.16	0.19	0.61	0.53	0.46	0.48	0.29	0.21	0.22	0.59	0.58
P2O5	<0.01	0.05	0.09	0.03	0.01	0.02	0.17	0.16	0.09	0.12	0.05	<0.01	0.02	0.19	0.18
MnO	0.03	0.04	0.05	0.02	0.02	0.02	0.06	0.05	0.05	0.05	0.03	0.02	0.02	0.04	0.04
Cr2O3	0.003	0.002	0.002	0.002	0.004	0.003	0.007	0.002	0.003	0.003	0.003	0.004	0.003	0.001	0.002
L.O.I.	0.4	0.5	0.3	0.6	0.6	0.6	0.4	0.8	0.5	0.5	0.6	1.3	0.8	1.6	1.7
Total	100.01	99.89	99.91	99.99	99.92	99.90	99.75	99.79	99.79	99.81	99.81	99.91	99.91	99.73	99.83
F	0.417	0.428	0.128	0.259	0.540	0.564	0.125	0.279	0.169	0.192	0.212	0.445	0.390	0.048	0.047
Mo	3.4	11.2	0.6	0.7	1.2	4.7	1.8	1.5	2.2	1.0	0.6	0.9	0.8	0.1	0.2
Cu	2.9	2.6	3.4	4.6	5.0	4.3	10.2	29.3	7.7	15.2	10.3	3.7	4.4	3.1	3.6
Pb	27.2	30.1	15.7	17.6	19.0	35.0	13.5	7.8	15.7	14.2	8.7	12.9	11.2	2.7	2.5
Zn	6	31	45	16	67	71	97	68	91	79	77	54	68	26	27
Ni	2.2	2.0	2.6	3.3	3.3	2.8	3.0	2.6	3.6	3.0	4.9	3.4	4.8	3.3	3.2
As	0.9	1.0	0.9	1.6	7.2	8.6	5.0	55.1	7.7	7.9	15.5	4.6	5.0	1.3	1.7
Cd	<0.1	<0.1	0.1	<0.1	0.1	0.1	0.2	0.2	0.2	0.3	0.1	<0.1	0.1	<0.1	<0.1
Sb	0.1	0.1	0.1	0.2	0.2	0.2	0.1	0.1	0.1	0.1	0.1	0.1	0.1	0.1	0.2
Bi	<0.1	<0.1	0.1	0.1	0.2	0.9	0.3	0.7	0.3	0.8	2.5	<0.1	0.5	<0.1	0.1
Ag	<0.1	<0.1	<0.1	<0.1	0.1	0.1	0.1	0.1	0.1	0.1	0.1	0.1	0.1	<0.1	<0.1
Au	<0.5**	<0.5**	0.8**	<0.5**	0.6**	3.6**	1.6**	1.9**	0.8**	<0.5**	2.4**	<0.5**	<0.5**	<0.5**	<0.5**
Hg	0.01	<0.01	<0.01	<0.01	0.01	<0.01	<0.01	0.01	<0.01	0.01	0.01	<0.01	0.01	0.01	0.01
Tl	0.2	0.4	0.3	0.3	0.7	0.6	0.2	0.5	0.3	0.2	0.6	0.6	0.5	<0.1	<0.1
Se	<0.5	<0.5	<0.5	<0.5	0.9	0.8	0.6	0.6	<0.5	0.7	0.5	0.7	0.7	0.6	<0.5

	Götemar		Tindered		Lovisa									Laisvall	
	Kr 0417	Kr 0418	Ti 0419	Ti 0420	Me 0401	Me 0402	Me 0403	Me 0408	Me 0404	Me 0409	Hv 0405	Hv 0406	Te 0407*	Ak 0415	Ak 0421
Sc	5	8	9	4	3	3	10	8	7	7	5	2	4	11	10
Ba	137.1	612.5	640.6	213.9	224.0	373.1	1,145.8	939.3	1,046.0	1,238.5	1,208.6	147.8	330.4	1,818.5	1,236.8
Be	10	10	7	5	9	7	4	6	5	4	5	6	6	7	3
Co	0.7	1.3	3.5	1.9	1.0	0.9	4.7	3.6	2.7	2.6	2.1	1.6	1.8	2.9	3.6
Cs	4.0	3.2	3.5	3.9	13.6	10.9	1.8	18.0	5.1	5.5	19.5	6.4	8.0	0.4	1.6
Ga	23.3	24.4	20.0	18.7	25.9	26.1	27.7	26.1	22.9	23.6	24.9	24.9	24.1	24.7	23.4
Hf	4.4	8.9	8.7	7.7	13.7	13.9	18.0	15.2	13.2	14.3	10.9	15.9	14.4	11.2	10.7
Nb	57.8	39.6	19.3	20.7	34.9	36.3	25.1	26.1	25.5	25.1	18.0	30.8	29.1	17.8	19.0
Rb	462.0	415.5	241.0	277.9	415.9	388.8	180.1	262.0	230.0	220.4	291.2	397.8	372.9	148.6	149.5
Sn	3	3	5	4	13	8	4	14	7	8	18	6	6	4	4
Sr	45.6	127.7	95.5	29.3	33.5	53.7	256.0	194.0	146.0	158.9	137.1	30.2	45.0	131.5	150.5
Ta	2.5	1.5	1.8	1.9	3.3	3.1	1.5	1.7	1.5	1.5	1.3	1.8	2.3	1.1	1.4
Th	47.3	63.5	21.6	50.3	56.4	55.1	20.2	26.2	19.3	19.3	22.4	91.5	49.8	19.9	20.4
U	16.6	14.2	7.4	16.6	14.8	15.5	4.8	6.2	5.0	6.1	5.9	15.5	13.8	6.3	12.0
V	<5	9	13	<5	7	6	12	7	8	6	<5	<5	<5	13	13
W	1.7	0.8	1.5	0.9	6.6	4.6	1.6	5.3	2.9	1.8	19.5	1.7	2.2	1.1	2.0
Zr	95.1	282.2	276.6	198.9	315.4	355.9	608.3	496.1	425.8	456.7	336.5	410.2	384.8	330.6	318.8
Y	15.8	31.6	75.4	84.3	119.0	122.8	70.6	69.3	69.9	66.5	56.4	90.0	103.1	96.5	56.4
La	59.6	115.1	49.1	80.1	128.2	142.0	79.3	84.1	72.3	69.8	69.8	187.2	142.6	73.7	55.9
Ce	91.9	219.0	105.9	181.9	284.7	315.2	184.1	190.5	166.8	157.0	149.0	416.9	324.0	183.7	123.9
Pr	7.35	20.30	12.39	18.86	30.78	33.88	21.30	21.62	19.22	18.49	16.53	42.64	34.24	21.57	14.29
Nd	20.3	61.1	47.1	61.3	101.1	110.3	78.3	79.2	70.6	67.8	57.9	134.6	112.5	80.6	51.8
Sm	2.5	8.8	10.1	12.1	18.9	21.0	15.5	14.8	14.2	13.7	11.3	22.7	19.8	19.1	10.3
Eu	0.52	1.53	1.54	0.65	0.79	1.01	2.92	2.35	2.26	2.46	2.26	0.85	0.96	3.91	1.87
Gd	1.58	5.49	9.97	9.86	14.78	16.34	12.23	11.36	11.37	11.22	9.04	15.52	15.16	17.95	8.75
Tb	0.27	0.82	1.81	1.89	2.79	3.02	2.02	2.02	1.90	1.86	1.64	2.56	2.71	2.93	1.56
Dy	1.56	4.56	11.18	11.74	16.20	17.82	11.88	11.87	11.45	11.09	9.32	14.22	15.77	15.40	8.91
Ho	0.39	0.91	2.53	2.63	3.57	3.85	2.50	2.40	2.40	2.32	1.92	2.89	3.32	3.12	1.91
Er	1.37	2.83	7.61	8.17	10.90	11.60	7.16	7.06	6.84	6.55	5.51	8.24	9.92	8.56	5.47
Tm	0.25	0.46	1.17	1.28	1.80	1.78	1.02	1.05	1.01	0.99	0.85	1.23	1.49	1.18	0.78
Yb	2.47	3.52	8.12	8.30	11.33	11.55	6.70	6.83	6.48	6.66	5.30	8.07	9.35	7.08	5.14
Lu	0.52	0.63	1.30	1.28	1.88	1.77	1.04	1.04	1.02	0.97	0.89	1.22	1.47	1.10	0.84

Major element oxides and F are given as weight percent, trace elements as ppm.
*Average of two analyses except for F.
**ppb